Chapter 10: Rheometry

CM4650
Polymer Rheology
Michigan Tech

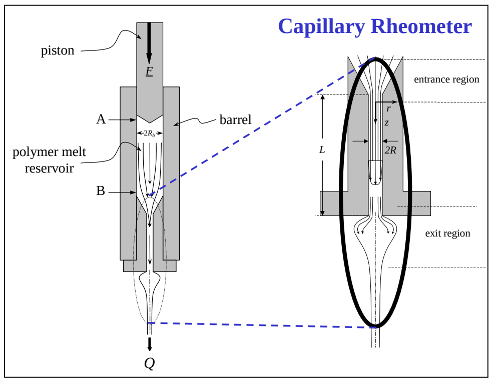

Advanced Const Modeling 2014 1

Rheometry (Chapter 10)

measurement

All the comparisons we have discussed require that we somehow measure the material functions on actual fluids.

TA Instruments
Anton Paar
Malvern
Brookfield
Thermo Scientific
Xpansion Instruments
Xpand Your Capabilities
RheoSense, Inc.
ATS RheoSystems
LS Instruments
Göttfert
Cambridge Polymer Group, Inc
BiolinScientific

2

Tactic: Divide the Problem in half

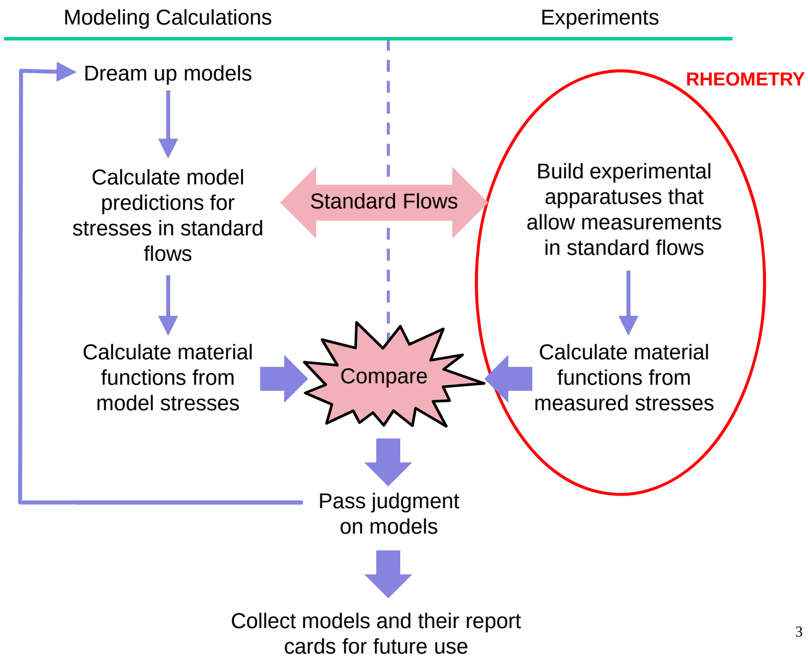

3

Standard Flows Summary

Choose velocity field: Symmetry of flow alone implies:

$$\underline{v} \equiv \begin{pmatrix} \dot{\varsigma}(t)x_2 \\ 0 \\ 0 \end{pmatrix}_{123} \qquad \underline{\underline{\tau}} = \begin{pmatrix} \tau_{11} & \tau_{12} & 0 \\ \tau_{21} & \tau_{22} & 0 \\ 0 & 0 & \tau_{33} \end{pmatrix}_{123}$$

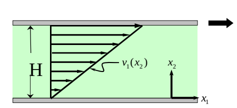

$$\underline{v} = \begin{pmatrix} -\frac{1}{2}\dot{\varepsilon}(t)(1+b)x_1 \\ -\frac{1}{2}\dot{\varepsilon}(t)(1-b)x_2 \\ \dot{\varepsilon}(t)x_3 \end{pmatrix}_{123} \qquad \underline{\underline{\tau}} = \begin{pmatrix} \tau_{11} & 0 & 0 \\ 0 & \tau_{22} & 0 \\ 0 & 0 & \tau_{33} \end{pmatrix}_{123}$$

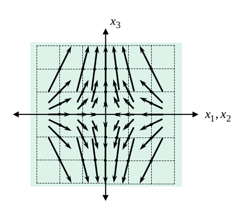

To measure the stresses we need for material functions, we must **produce** the defined flows

4

Simple Shear flow (Drag)

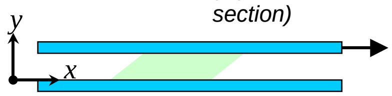

$$\underline{v} \equiv \begin{pmatrix} \dot{\varsigma}(t)x_2 \\ 0 \\ 0 \end{pmatrix}_{123}$$

Challenges:

- •Sample loading
- •Maintain parallelism
- •Producing linear motion
- •Stress measurement (Edge effects)
- •Signal strength

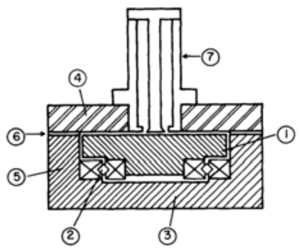

Fig. 2. Cross section of the sliding plate rheometer, showing the moving plate [1], linear bearing [2], back plate, [3], stationary plate [4], side supports [5], and shims [6]. (Details, e.g. such as assembly bolts, etc. not shown.)

From the McGill website (2006): Hee Eon Park, first-year postdoc in Chemical Engineering, works on a high-pressure sliding plate rheometer, the only instrument of its kind in the world.

Interlaken Technology

J. M. Dealy and S. S. Soong "A Parallel Plate Melt Rheometer Incorporating a Shear Stress Transducer,"J. Rheol. 28, 355 (1984)

5

Although we stipulated simple, homogeneous shear flow be produced throughout the flow domain, can we, perhaps, relax that requirement?

$$\underline{v} \equiv \begin{pmatrix} \dot{\varsigma}(t)x_2 \\ 0 \\ 0 \end{pmatrix}_{123}$$

6

Viscometric flow: motions that are locally equivalent to steady simple shearing motion at every particle

- •globally steady with respect to some frame of reference
- •streamlines that are straight, circular, or helical
- •each flow can be visualized as the relative motion of a sheaf of material surfaces (slip surfaces)
- •each slip surface moves without changing shape during the motion
- •every particle lies on a material surface that moves without stretching (inextensible slip surfaces)

Viscometric Flows:
1. Steady tube flow
2. Steady tangential annular flow
3. Steady torsional flow (parallel plate flow)
4. Steady cone-and-plate flow (small cone angle)
5. Steady helical flow

Wan-Lee Yin, Allen C. Pipkin, "Kinematics of viscometric flow," *Archive for Rational Mechanics and Analysis,* 37(2) 111-135, 1970
R. B. Bird, R. Armstrong, O. Hassager, *Dynamics of Polymeric Liquids*, 2nd edition, Wiley (1986), section 3.7.

7

Experimental Shear Geometries (viscometric flows)

Viscometric Flows:
1. Steady tube flow
2. Steady tangential annular flow
3. Steady torsional pp flow
4. Steady cone-and-plate flow
5. ~~Steady helical flow~~

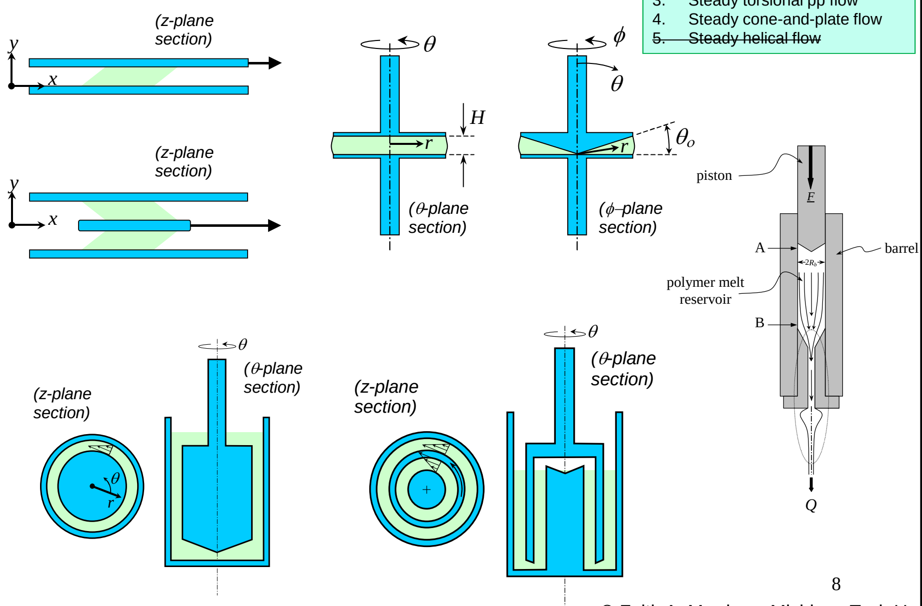

8

Types of Shear Rheometry

Mechanical:

•Mechanically produce **linear drag flow**;
Measure (shear strain transducer):
Shear stress on a surface

1. planar Couette

•Mechanically produce **torsional drag flow**;
Measure: (strain-gauge; force rebalance)
Torque to rotate surfaces
Back out material functions

1. cone and plate;
2. parallel plate;
3. circular Couette

•Produce **pressure-driven flow** through conduit
Measure:
Pressure drop/flow rate
Back out material functions

1. capillary flow
2. slit flow

9

Capillary Rheometer

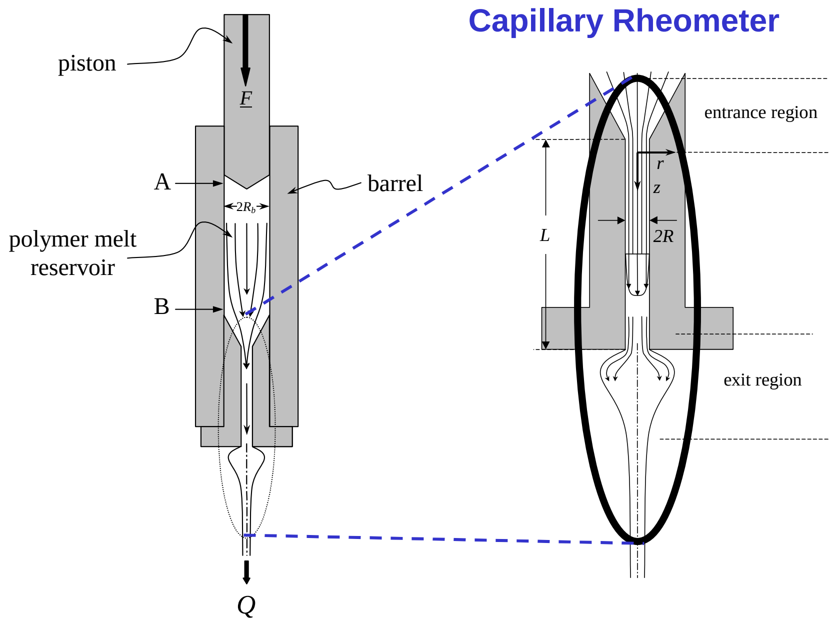

10

Capillary Rheometer

The basics

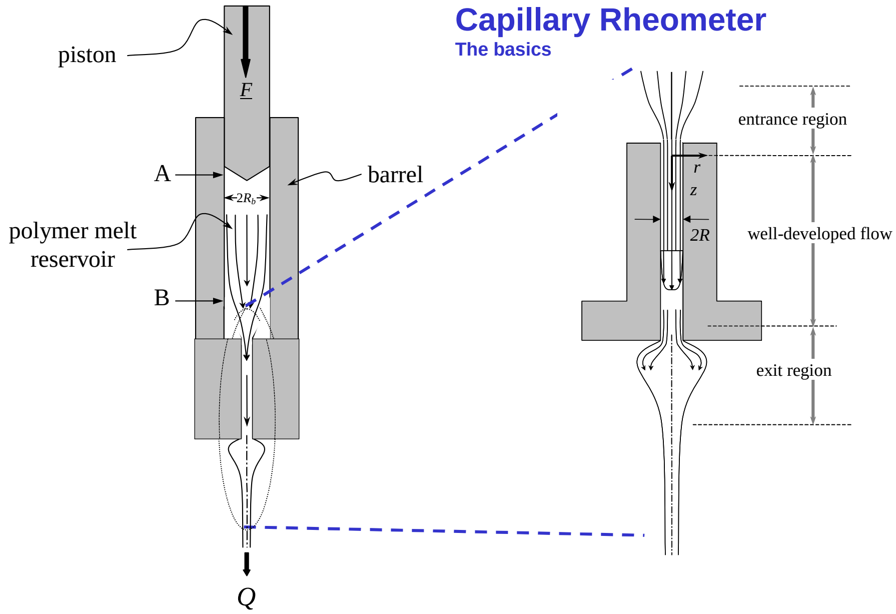

11

Exercise:

• What is the shear stress in capillary flow, for a fluid with unknown constitutive equation?

•What is the shear rate in capillary flow?

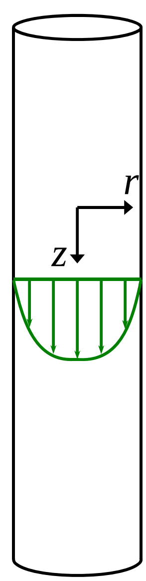

12

To calculate shear rate, shear stress, look at EOM:

$$\eta = \frac{\tau_R}{\dot{\gamma}_R}$$

$$P \equiv p - \rho g z$$

$$\rho\left(\cancel{\frac{\partial \underline{v}}{\partial t}} + \cancel{\underline{v}\cdot\nabla\underline{v}}\right) = -\nabla P - \nabla\cdot\underline{\underline{\tau}}$$

steady state

unidirectional

Assume:
- Incompressible fluid
- no θ-dependence
- long tube
- symmetric stress tensor
- Isothermal
- Viscosity indep of pressure

$$\begin{pmatrix} 0 \\ 0 \\ 0 \end{pmatrix}_{r\theta z} = \begin{pmatrix} -\frac{\partial P}{\partial r} \\ 0 \\ -\frac{\partial P}{\partial z} \end{pmatrix}_{r\theta z} - \begin{pmatrix} \frac{1}{r}\frac{\partial r\tau_{rr}}{\partial r} - \frac{\tau_{\theta\theta}}{r} \\ \frac{1}{r^2}\frac{\partial r^2\tau_{r\theta}}{\partial r} \\ \frac{1}{r}\frac{\partial r\tau_{rz}}{\partial r} \end{pmatrix}_{r\theta z}$$

13

Shear stress in capillary flow:

$$\boxed{\tau_{rz} = \frac{(P_0 - P_L)r}{2L} = \tau_R \frac{r}{R}} \quad \left(\frac{\partial P}{\partial z} = \text{constant}\right)$$

(varies with position, i.e. inhomogeneous flow)

What was the shear stress in drag flow?

14

Viscosity from capillary flow – inhomogeneous shear flow

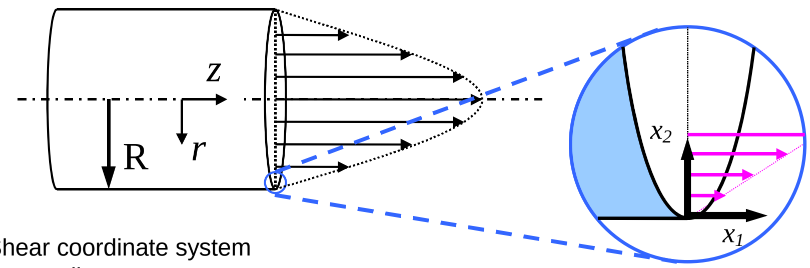

Shear coordinate system near wall:

$$\hat{e}_1 = \hat{e}_z$$
$$\hat{e}_2 = -\hat{e}_r$$
$$\hat{e}_3 = -\hat{e}_\theta$$

$$\tau_{21} = -\tau_{rz}\big|_{r=R} \equiv -\tau_R$$

$$\dot{\gamma}_0 = \frac{\partial v_z}{\partial(-r)} = -\frac{\partial v_z}{\partial r} = \dot{\gamma}\big|_{r=R} \equiv \dot{\gamma}_R$$

$$\boxed{\eta = \frac{-\tau_{21}}{\dot{\gamma}_0} = \frac{\tau_R}{\dot{\gamma}_R}}$$

wall shear stress

wall shear rate

It is not the same shear rate everywhere, but if we focus on the wall we can still get $\eta(\dot{\gamma}_R)$

15

Viscosity from Wall Stress/Shear rate

Note: we are assuming no-slip at the wall

Wall shear stress in capillary flow:

$$\boxed{\tau_{rz}\big|_{r=R} = \frac{(P_0 - P_L)r}{2L}\bigg|_{r=R} = \frac{\Delta P R}{2L}}$$

$$\left(\frac{\partial P}{\partial z} = \text{constant}\right)$$

What is shear rate at the wall in capillary flow?

$$\dot{\gamma} = \frac{\partial v_z}{\partial(-r)} = -\frac{\partial v_z}{\partial r} = \dot{\gamma}\big|_{r=R} \equiv \dot{\gamma}_R$$

If $v_z(r)$ is known, this is easy to calculate.

16

Velocity fields, Flow in a Capillary

Newtonian fluid:

$$v_z(r) = \frac{2Q}{\pi R^2}\left[1-\left(\frac{r}{R}\right)^2\right]$$

Power-law GNF fluid:

$$v_z(r) = R^{\frac{1}{n}+1}\left(\frac{P_0 - P_L}{2mL}\right)^{\frac{1}{n}}\left(\frac{1}{1/n+1}\right)\left[1-\left(\frac{r}{R}\right)^{\frac{1}{n}+1}\right]$$

17

Wall shear-rate for a Newtonian fluid

Hagen-Poiseuille:

$$Q = \frac{\pi \Delta P R^4}{8\mu L}$$

$$\frac{4Q}{\pi R^3} = \frac{1}{\mu}\frac{\Delta P R}{2L}$$

$$\dot{\gamma}_a = \frac{4Q}{\pi R^3}$$

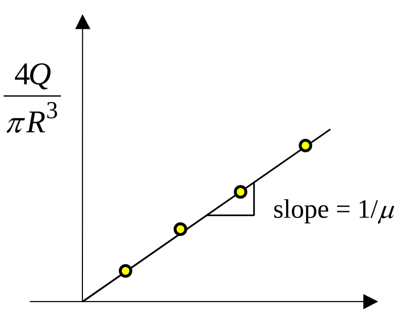

$$\tau_R = \frac{\Delta P R}{2L}$$

18

Wall shear-rate for a Power-law GNF

PL-GNF flow rate:

$$Q = \left(\frac{\Delta P R}{2L}\right)^{\frac{1}{n}} \frac{1}{m^{1/n}} \frac{n\pi R^3}{1+3n}$$

$$\dot{\gamma}_a = \frac{4Q}{\pi R^3}$$

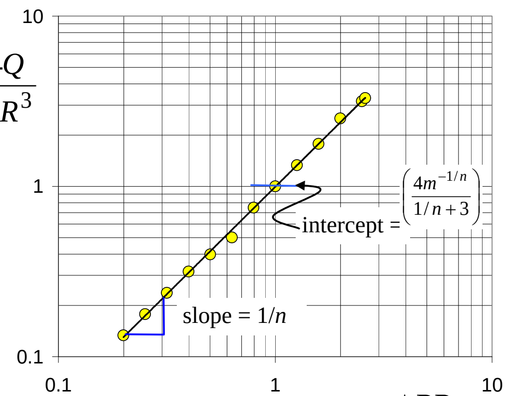

$$\tau_R = \frac{\Delta P R}{2L}$$

For an unknown, non-Newtonian fluid, we need to take special steps to determine the wall shear rate

The wall shear rate is generally greater than for a Newtonian fluid.

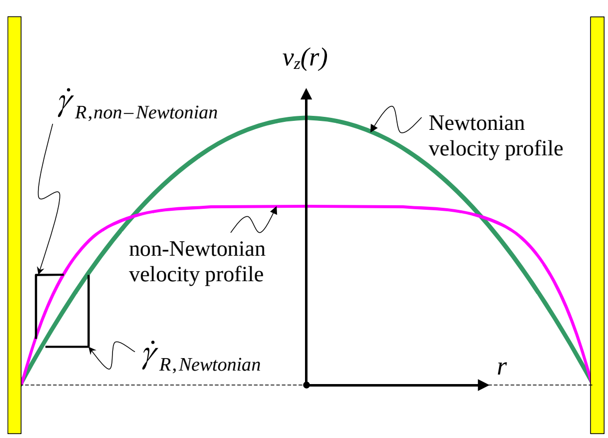

For a General non-Newtonian fluid

$$Q = ?$$

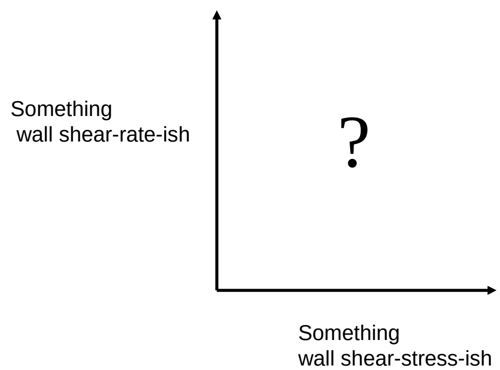

21

Weissenberg-Rabinowitsch correction

$$\boxed{\dot{\gamma}_R(\tau_R) = \frac{4Q}{\pi R^3}\left[\frac{1}{4}\left(3 + \frac{d\ln\dot{\gamma}_a}{d\ln\tau_R}\right)\right]}$$

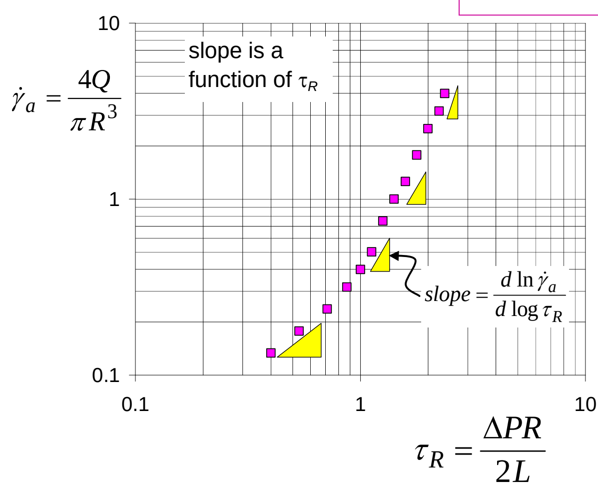

22

Capillary flow

Assumptions:

- •Steady……………………………•No intermittent flow allowed
- •θ symmetry……………………•No spiraling flow allowed
- •Unidirectional …………………•Check end effects
- •Incompressible………………•Avoid high absolute pressures
- •Constant pressure gradient…•Check end effects
- •No slip…………………………•Check wall slip

Methods have been devised to account for
•Slip
•End effects

23

Slip at the wall - Mooney analysis

Slip at the wall reduces the shear rate near the wall.

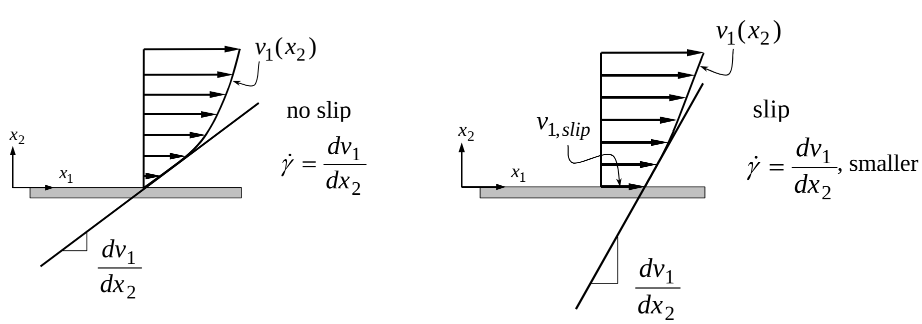

24

Slip at the wall - Mooney analysis

Slip at the wall reduces the shear rate near the wall.

$$v_{z,true} = v_{z,measured} - v_{z,slip}$$

$$v_{z,av} = \frac{Q}{\pi R^2}$$

$$\frac{4v_{z,av}}{R} = \frac{4Q}{\pi R^3} = \dot{\gamma}_a$$

$$\dot{\gamma}_{a,slip-corrected} \equiv \frac{4v_{z,av}}{R} - \frac{4v_{z,slip}}{R}$$

$$\frac{4v_{z,av}}{R} = \underbrace{4v_{z,slip}}_{\text{slope}}\left(\frac{1}{R}\right) + \dot{\gamma}_{a,slip-corrected}$$

intercept

$$\frac{4v_{z,av}}{R} = \frac{4Q_{measured}}{\pi R^3}$$

At constant wall shear stress, take data in capillaries of various R

The Mooney correction is a correction to the apparent shear rate

25

Slip at the wall - **Mooney analysis**

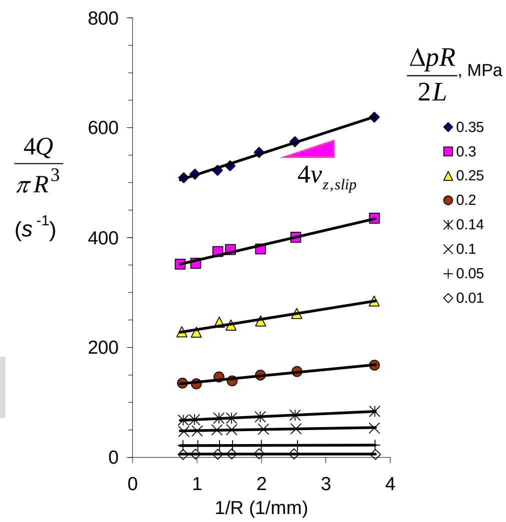

Note: each line is at constant wall shear stress (data may need to be interpolated to meet this requirement).

Turns out there is slip sometimes!

Figure 10.10, p. 396 Ramamurthy, LLDPE

26

Entrance and exit effects - Bagley correction

The pressure gradient is not accurately represented by the raw pressure drop: $\dfrac{P_{reservoir} - P_{atm}}{L}$

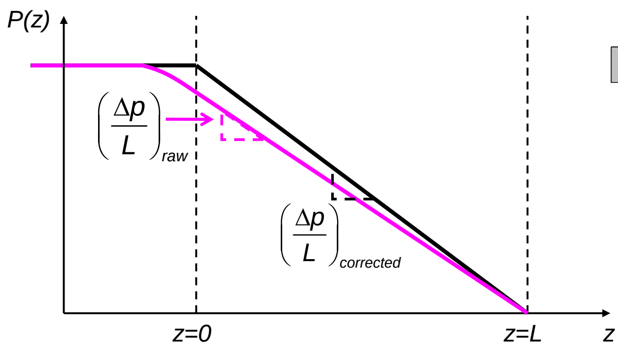

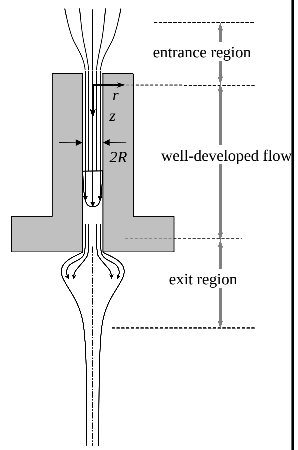

27

Entrance and exit effects - Bagley correction

$$\tau_R = \frac{\Delta P R}{2L} \Rightarrow \Delta P = \left(2\tau_R\right)\frac{L}{R}$$

Constant at constant Q

Run for different capillaries

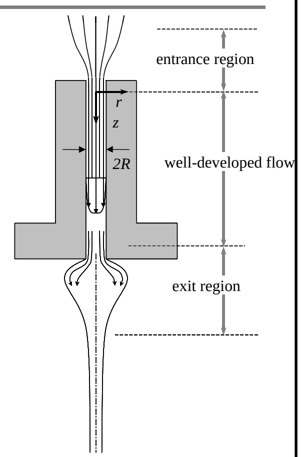

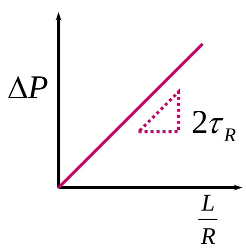

This is the result when the end effects are negligible.

The Bagley correction is a correction to the wall shear stress

28

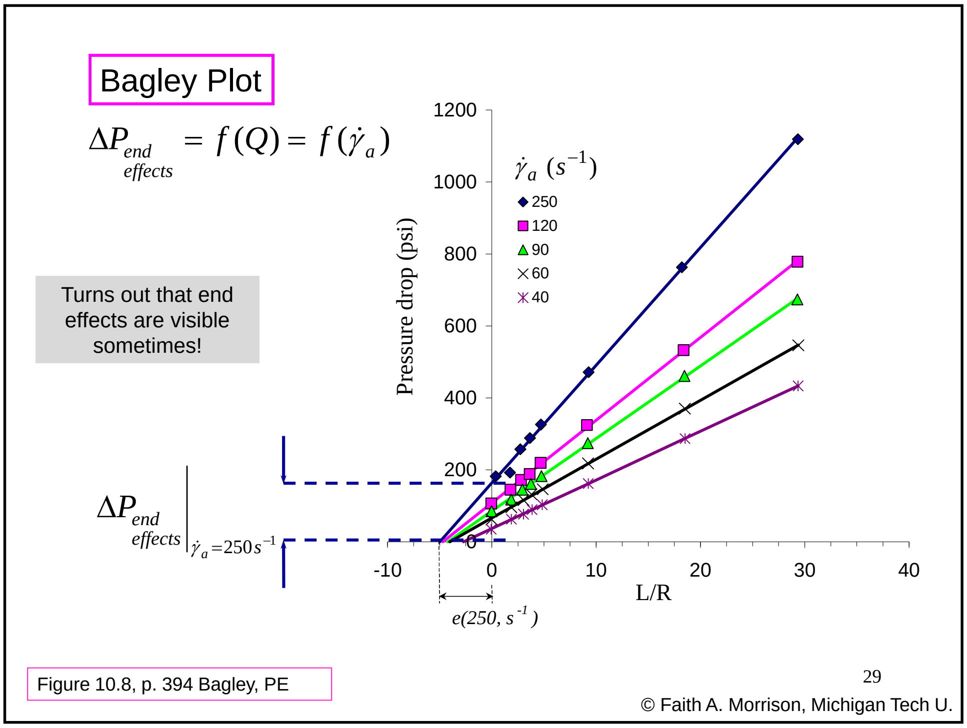
Bagley Plot
$\Delta P_{\substack{end \\ effects}} = f(Q) = f(\dot{\gamma}_a)$
Turns out that end effects are visible sometimes!
$\Delta P_{\substack{end \\ effects}}\Big|_{\dot{\gamma}_a = 250 s^{-1}}$
Pressure drop (psi)
L/R
$\dot{\gamma}_a\ (s^{-1})$
250
120
90
60
40
$e(250, s^{-1})$
Figure 10.8, p. 394 Bagley, PE
29
© Faith A. Morrison, Michigan Tech U.

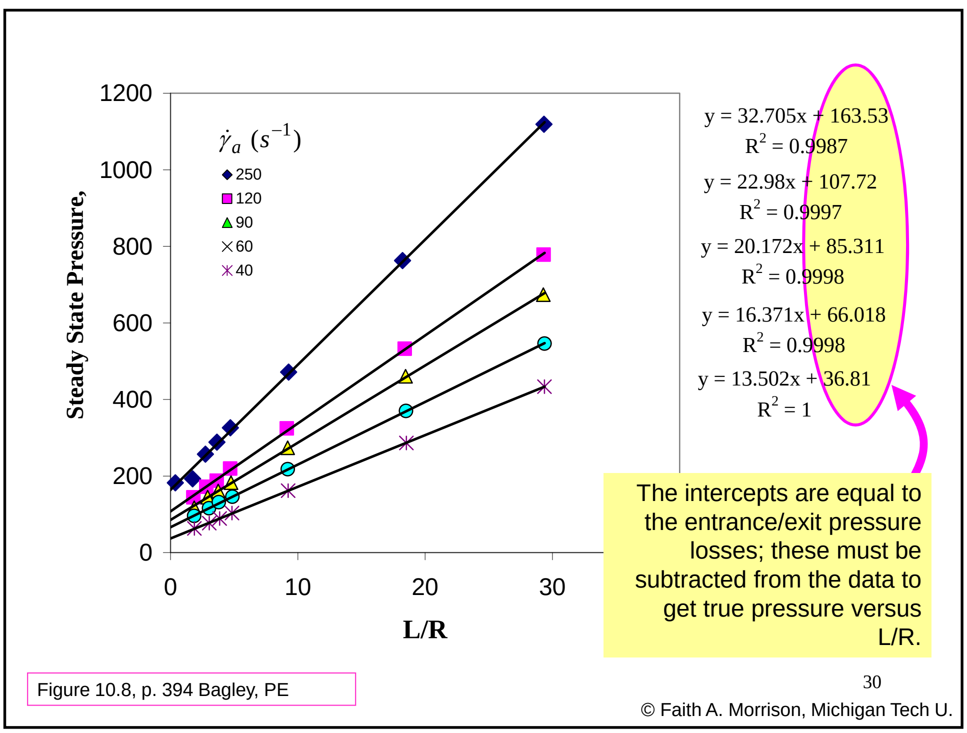
Steady State Pressure,
L/R
$\dot{\gamma}_a\ (s^{-1})$
250
120
90
60
40
y = 32.705x + 163.53
R^2 = 0.9987
y = 22.98x + 107.72
R^2 = 0.9997
y = 20.172x + 85.311
R^2 = 0.9998
y = 16.371x + 66.018
R^2 = 0.9998
y = 13.502x + 36.81
R^2 = 1
The intercepts are equal to the entrance/exit pressure losses; these must be subtracted from the data to get true pressure versus L/R.
Figure 10.8, p. 394 Bagley, PE
30
© Faith A. Morrison, Michigan Tech U.

Figure 10.8, p. 394 Bagley, PE

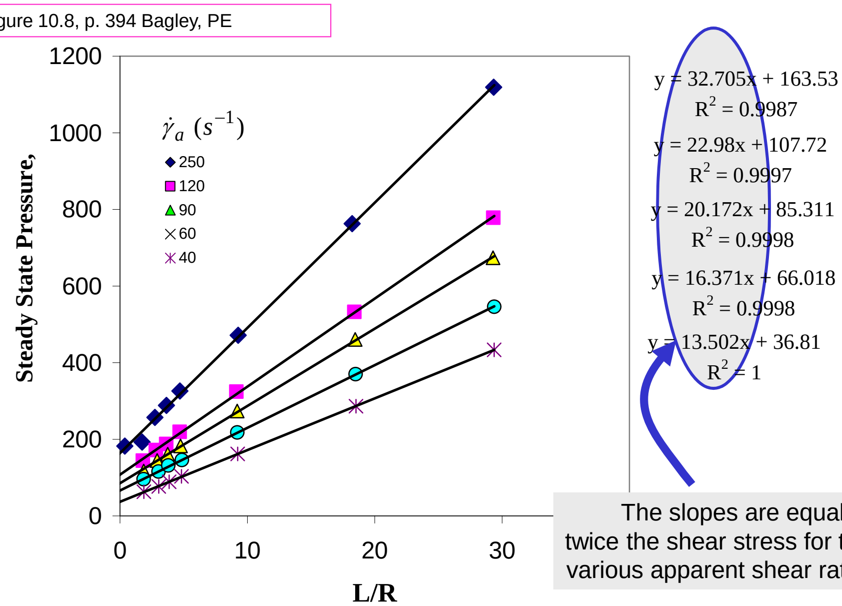

The slopes are equal to twice the shear stress for the various apparent shear rates

$$\tau_{rz} = \frac{\Delta p R}{2L} \quad \Rightarrow \quad \Delta p = 2\tau_{rz}\left(\frac{L}{R}\right)$$

The data so far:

$\dot{\gamma}_a$	ΔP_{ent}		τ_R	τ_R
gammdotA (1/s)	deltPent psi	slope psi	sh stress psi	sh stress Pa
250	163.53	32.705	16.3525	1.1275E+05
120	107.72	22.98	11.49	7.9220E+04
90	85.311	20.172	10.086	6.9540E+04
60	66.018	16.371	8.1855	5.6437E+04
40	36.81	13.502	6.751	4.6546E+04

Now, turn apparent shear rate into wall shear rate (correct for non-parabolic velocity profile).

Figure 10.8, p. 394 Bagley, PE

Weissenberg-Rabinowitsch correction

$$\dot{\gamma}_R(\tau_R) = \frac{4Q}{\pi R^3}\left[\frac{1}{4}\left(3 + \frac{d\ln\dot{\gamma}_a}{d\ln\tau_R}\right)\right]$$

$$\dot{\gamma}_a = \frac{4Q}{\pi R^3}$$

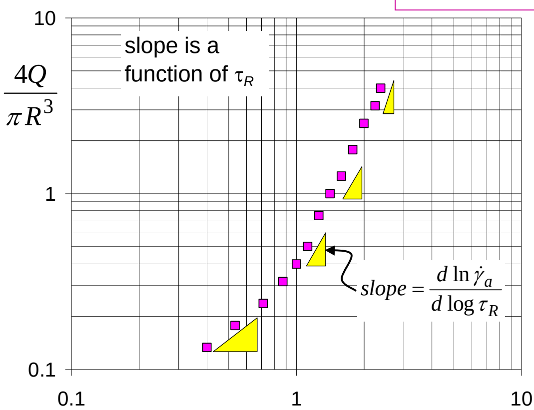

$$\tau_R = \frac{\Delta PR}{2L}$$

Sometimes the WR correction varies from point-to-point; sometimes it is a constant that applies to all data points (PL region).

33

Weissenberg-Rabinowitsch correction

$$\frac{d\ln\dot{\gamma}_a}{d\ln\tau_R} = 2.0677$$

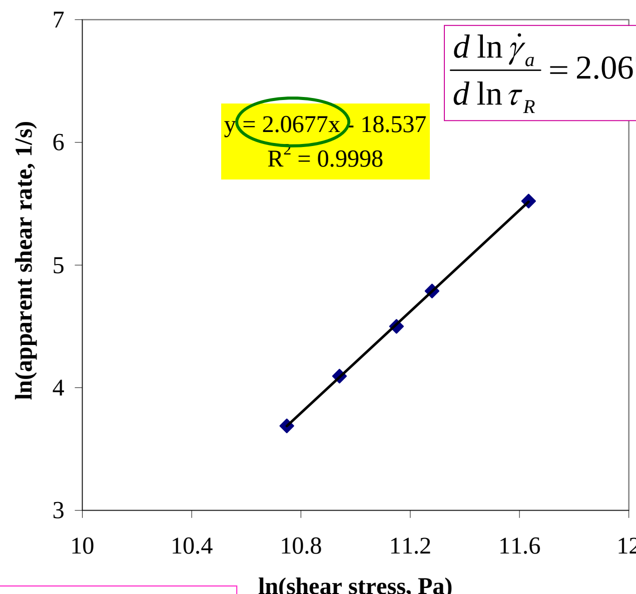

This slope is usually >1

Figure 10.8, p. 394 Bagley, PE

34

The data corrected for entrance/exit and non-parabolic velocity profile:

$$\eta = \frac{\tau_R}{\dot{\gamma}_R}$$

$\dot{\gamma}_a$ gammdotA (1/s)	ΔP_{ent} deltPent psi	ΔP_{ent} deltPent Pa	τ_R sh stress Pa	ln(sh st)	ln(gda)	WR correction	$\dot{\gamma}_R$ gam-dotR 1/s	viscosity Pa s
250	163.53	1.1275E+06	1.1275E+05	11.63289389	5.521460918	2.0677	316.73125	3.5597E+02
120	107.72	7.4270E+05	7.9220E+04	11.2799902	4.787491743	2.0677	152.031	5.2108E+02
90	85.311	5.8820E+05	6.9540E+04	11.14966143	4.49980967	2.0677	114.02325	6.0988E+02
60	66.018	4.5518E+05	5.6437E+04	10.9408774	4.094344562	2.0677	76.0155	7.4244E+02
40	36.81	2.5380E+05	4.6546E+04	10.74820375	3.688879454	2.0677	50.677	9.1849E+02

Now, plot viscosity versus wall-shear-rate

Figure 10.8, p. 394 Bagley, PE

35

Viscosity of polyethylene from Bagley's data

$$\eta = \frac{\tau_R}{\dot{\gamma}_R}$$

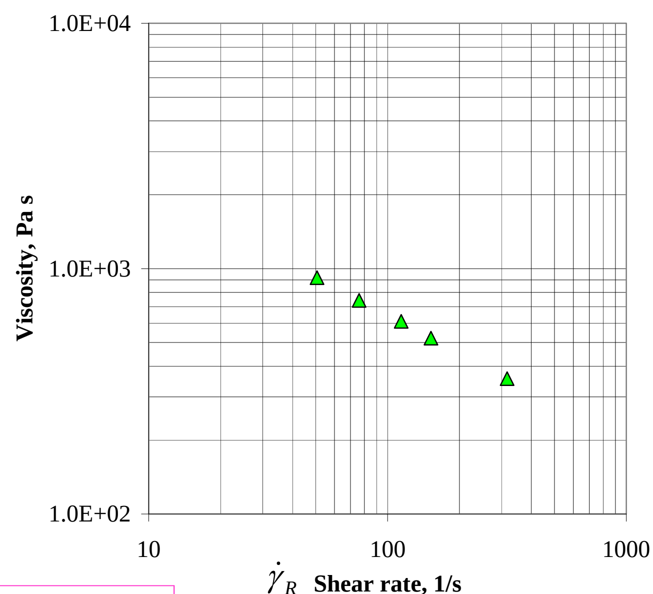

Figure 10.8, p. 394 Bagley, PE

36

Viscosity from Capillary Experiments, Summary:

1. Take data of pressure-drop versus flow rate for capillaries of various lengths; perform Bagley correction on Δp (entrance pressure losses)
2. If possible, also take data for capillaries of different radii; perform Mooney correction on Q (slip)
3. Perform the Weissenberg-Rabinowitsch correction (obtain correct wall shear rate)
4. Plot true viscosity versus true wall shear rate
5. Calculate power-law *m*, *n* from fit to final data (if appropriate)

raw data: $\Delta P(Q)$

final data: $\eta = \tau_R / \dot{\gamma}_R$

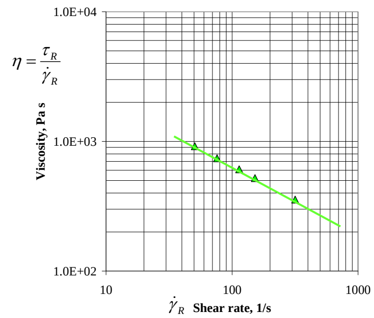

37

What about the shear normal stresses, Ψ_1, Ψ_2 from capillary data?

Extrudate swell - relation to N_1 is model dependent (see discussion in Macosko, p254)

$$N_1^2 = 8\tau_R^2\left(\left(\frac{D_e}{2R}\right)^6 - 1\right)$$

Assuming unconstrained recovery after steady shear, K-BKZ model with one relaxation time

$D_e =$ Extrudate diameter

Not a great method; can perhaps be used to index materials

Ψ_2 ? (cannot obtain from capillary flow, but…)

Macosko, Rheology: *Principles, Measurements, and Applications*, VCH 1994.

38

We can obtain Ψ_1, Ψ_2 from slit-flow data: **Hole Pressure-Error**

Pressure transducers mounted in an access channel (hole) do not measure the same pressure as those that are "flush-mounted":

$$\delta p_h \equiv p_{flush} - p_{hole}$$

Slot transverse to flow: $$N_1 = 2\delta p_h \left(\frac{d \ln \delta p_h}{d \ln \tau_w} \right)$$

Slot parallel to flow: $$N_2 = -\delta p_h \left(\frac{d \ln \delta p_h}{d \ln \tau_w} \right)$$

Circular hole: $$N_1 - N_2 = 3\delta p_h \left(\frac{d \ln \delta p_h}{d \ln \tau_w} \right)$$

Hou, Tong, deVargas, Rheol. Acta 1977, 16, 544

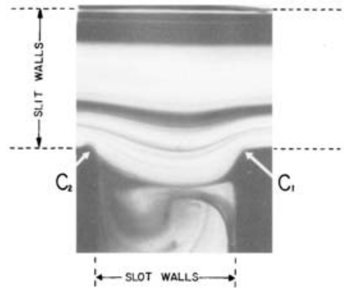

Fig. 4. Photograph of streamlines showing curvature near the mouth of a hole of slit cross-section for polyethylene (NPE 952) melts. Direction of flow is from right to left. Flow rate ≃ 0.02 ml/sec; shear rate at the wall ≃ 3.2 sec^{-1}; d = 0.05 in

(We can of course obtain η also from slit-flow data; the equations are analogous to the capillary flow equations)

Lodge, in *Rheological Measurement,* Collyer, Clegg, eds. Elsevier, 1988
Macosko, Rheology: *Principles, Measurements, and Applications*, VCH 1994.

39

Limits on Measurements: Flow instabilities in rheology

Flow driven by constant pressure

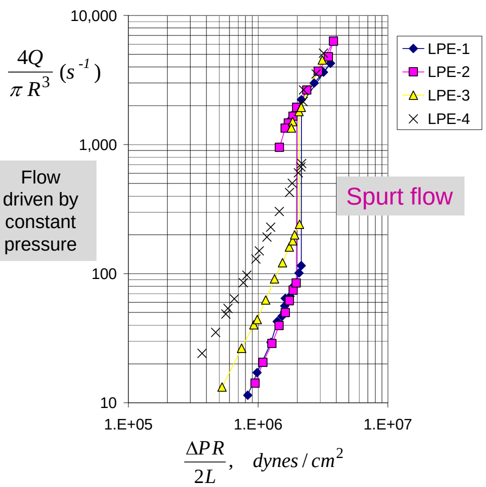

Figure 6.10, p. 177 Blyler and Hart; PE

capillary flow

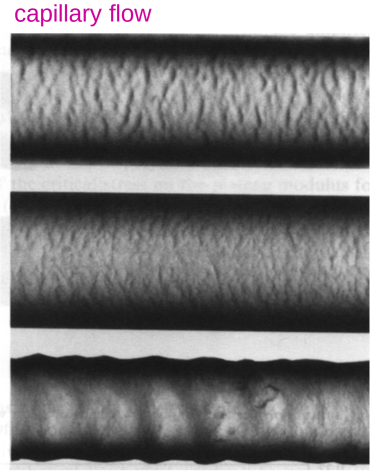

Figure 6.9, p. 176
Pomar et al. LLDPE

40

Limits on Measurements: Flow instabilities in rheology

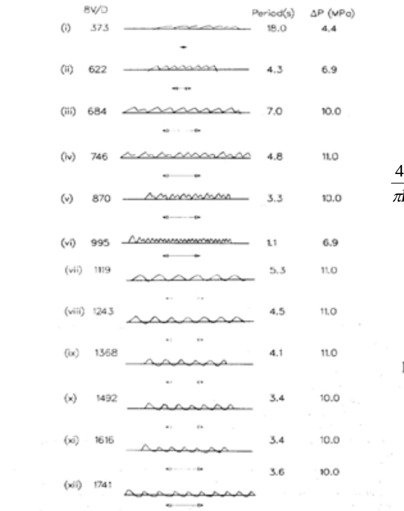

Fig. 11. Force vs. time curves; L/D = 100.1. Slip-stick region. The time interval indicated by the arrow below each curve equals ten seconds. Polymer was added to the reservoir after run (vi).

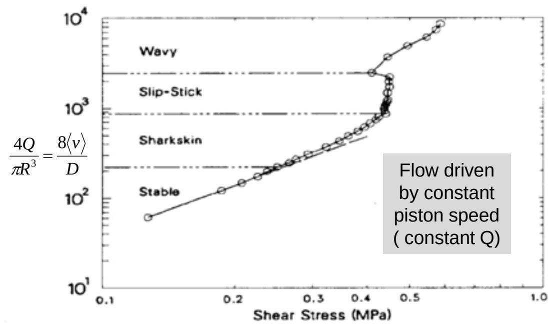

Fig. 2. Uncorrected capillary data for LLDPE at 215°C, L/D = 33.2.

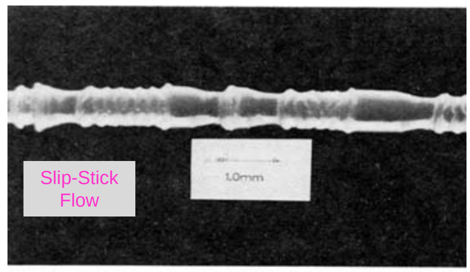

Fig. 8. LLDPE extrudate: transition region observed in slip–stick flow region. 8 V/D = 985; L/D = 100.1.

D. Kalika and M. Denn, *J. Rheol*. 31, 815 (1987)

Torsional Parallel Plates

Viscometric flow

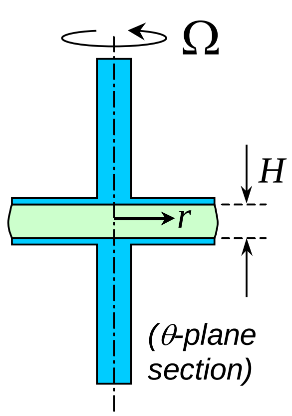

$$\underline{v} = \begin{pmatrix} 0 \\ v_\theta(r,z) \\ 0 \end{pmatrix}_{r\theta z}$$

42

To calculate shear rate:

$$\underline{v} = \begin{pmatrix} 0 \\ A(r)z + B(r) \\ 0 \end{pmatrix}_{r\theta z}$$

$$v_\theta = A(r)z + B(r)$$

$$v_\theta = \frac{r\Omega z}{H} \qquad \text{(due to boundary conditions)}$$

$$\dot{\gamma} = \left|\dot{\underline{\underline{\gamma}}}\right| = \left| \begin{pmatrix} 0 & \frac{\partial v_\theta}{\partial r} - \frac{v_\theta}{r} & 0 \\ \frac{\partial v_\theta}{\partial r} - \frac{v_\theta}{r} & 0 & \frac{\partial v_\theta}{\partial z} \\ 0 & \frac{\partial v_\theta}{\partial z} & 0 \end{pmatrix}_{r\theta z} \right|$$

$$\dot{\gamma} = ?$$

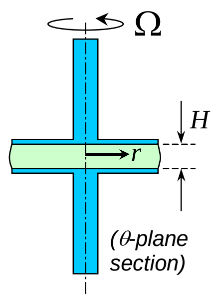

43

Result:

$$\underline{v} = \begin{pmatrix} 0 \\ \frac{r\Omega z}{H} \\ 0 \end{pmatrix}_{r\theta z} \qquad \dot{\gamma} = \frac{r\Omega}{H}$$

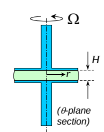

To calculate shear stress, look at EOM:

$$P \equiv p - \rho g z$$

$$\underline{\underline{\tau}} = \begin{pmatrix} \tau_{rr} & 0 & 0 \\ 0 & \tau_{\theta\theta} & \tau_{\theta z} \\ 0 & \tau_{z\theta} & \tau_{zz} \end{pmatrix}_{r\theta z}$$

(viscometric flow)

$$\rho\left(\cancel{\frac{\partial \underline{v}}{\partial t}} + \cancel{\underline{v}\cdot\nabla\underline{v}}\right) = -\nabla P - \nabla\cdot\underline{\underline{\tau}}$$

steady state — neglect inertia

$$\begin{pmatrix} 0 \\ 0 \\ 0 \end{pmatrix}_{r\theta z} = \begin{pmatrix} -\frac{\partial P}{\partial r} \\ 0 \\ -\frac{\partial P}{\partial z} \end{pmatrix}_{r\theta z} - \begin{pmatrix} \frac{1}{r}\frac{\partial r\tau_{rr}}{\partial r} - \frac{\tau_{\theta\theta}}{r} \\ \frac{\partial \tau_{z\theta}}{\partial z} \\ \frac{\partial \tau_{zz}}{\partial z} \end{pmatrix}_{r\theta z}$$

Assume:
- Form of velocity
- no θ-dependence
- symmetric stress tensor
- neglect inertia
- no slip
- isothermal

44

Result:

$$\frac{\partial \tau_{z\theta}}{\partial z} = 0$$

$$\tau_{z\theta} = f(r)$$

The experimentally measurable variable is the torque to turn the plate:

$$\underline{T} = \iint_S \left[\underline{R} \times \left(\hat{n} \cdot -\underline{\underline{\Pi}}\right)\right]_{surface} dS$$

$$\underline{T} = \int_0^{2\pi}\int_0^{R} \left[r\hat{e}_r \times \left(\hat{e}_z \cdot -\underline{\underline{\Pi}}\right)\right]_{z=H} r\,dr\,d\theta$$

$$T_z = 2\pi \int_0^R \left[-\tau_{z\theta}\right]_{z=H} r^2 dr$$

Following Rabinowitsch, replace stress with viscosity, r with shear rate, and differentiate.

Torsional Parallel-Plate Flow - Viscosity

Measureables:
Torque **T** to turn plate
Rate of angular rotation **Ω**

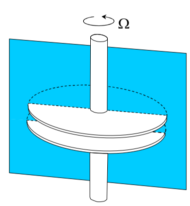

cross-sectional view:

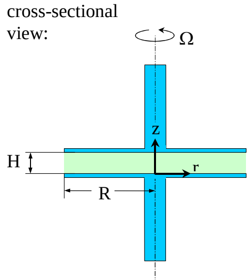

Note: shear rate experienced by fluid elements depends on their r position. (consider effect on complex fluids)

$$\dot{\gamma} = \frac{r\Omega}{H} = \dot{\gamma}_R \frac{r}{R}$$

By carrying out a Rabinowitsch-like calculation, we can obtain the stress at the rim (r=R).

$$\tau_{z\theta}\big|_{r=R} = -T/2\pi R^3 \left[3 + \frac{d\ln(T/2\pi R^3)}{d\ln\dot{\gamma}_R}\right]$$

$$\boxed{\eta(\dot{\gamma}_R) = \frac{-\tau_{z\theta}\big|_{r=R}}{\dot{\gamma}_R}}$$

Correction required

Torsional Parallel-Plate Flow - correction

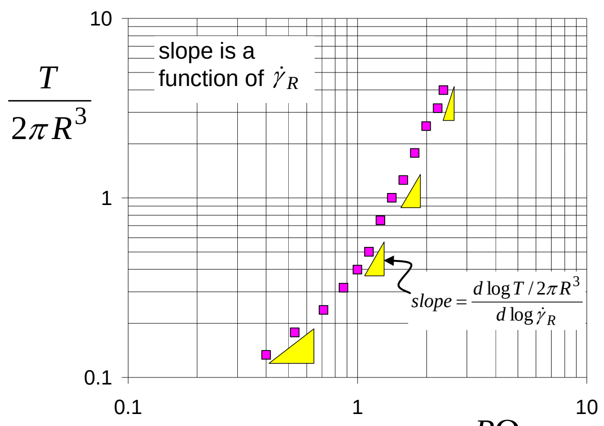

$$\dot{\gamma}_R = \frac{R\Omega}{H}$$

$$\eta(\dot{\gamma}_R) = \frac{T/2\pi R^3}{\dot{\gamma}_R}\left[3 + \frac{d\ln(T/2\pi R^3)}{d\ln\dot{\gamma}_R}\right]$$

47

Torsional Parallel-Plate Flow – Viscosity – Approximate method

$$\tau_{z\theta}\Big|_{r=R} = -T/2\pi R^3\left[3 + \frac{d\ln(T/2\pi R^3)}{d\ln\dot{\gamma}_R}\right]$$

=1 for Newtonian

$$-\tau_a \equiv \frac{2T}{\pi R^3}$$

For many materials: $\frac{d\ln(T/2\pi R^3)}{d\ln\dot{\gamma}_R} < 1.4$

$$\eta(\tau) = \eta_a(\tau_a) \pm 2\%$$

$$\tau = \tau_a(r = 0.76R)$$

Giesekus and Langer Rheol. Acta, 16, 1 1977

$$\eta(\dot{\gamma}_{0.96R}) = \frac{-\tau_{0.76R}}{\dot{\gamma}_{0.76R}}$$

No correction required

(but making a material assumption)

Macosko, Rheology: *Principles, Measurements, and Applications*, VCH 1994, p220

48

Torsional Parallel-Plate Flow – Normal Stresses

Similar tactics, logic (see Macosko, p221)

$$\left(N_1 - N_2\right)\Big|_{\dot{\gamma}_R} = \frac{F_z}{\pi R^2}\left[2 + \frac{d\ln(F_z)}{d\ln\dot{\gamma}_R}\right]$$

(Not a direct material funcion)

Macosko, Rheology: *Principles, Measurements, and Applications*, VCH 1994, p220

49

Torsional Cone and Plate

(spherical coordinates)

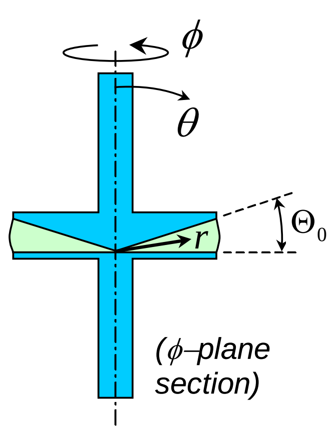

$$\underline{v} = \begin{pmatrix} 0 \\ 0 \\ v_\phi(r,\theta) \end{pmatrix}_{r\theta\phi}$$

50

To calculate shear rate:

$$\underline{v} = \begin{pmatrix} 0 \\ 0 \\ A(-r\theta)+B \end{pmatrix}_{r\theta\phi}$$

$$v_\phi = A(-r\theta)+B$$

$$v_\phi = \frac{r\Omega}{\Theta_0}\left(\frac{\pi}{2}-\theta\right)$$ (due to boundary conditions)

$$\dot{\gamma} = \left|\dot{\underline{\underline{\gamma}}}\right| = \left|\begin{pmatrix} 0 & 0 & r\frac{\partial}{\partial r}\left(\frac{v_\phi}{r}\right) \\ 0 & 0 & \frac{\sin\theta}{r}\frac{\partial}{\partial\theta}\left(\frac{v_\phi}{\sin\theta}\right) \\ r\frac{\partial}{\partial r}\left(\frac{v_\phi}{r}\right) & \frac{\sin\theta}{r}\frac{\partial}{\partial\theta}\left(\frac{v_\phi}{\sin\theta}\right) & 0 \end{pmatrix}_{r\theta\phi}\right|$$

$$\dot{\gamma} = ?$$

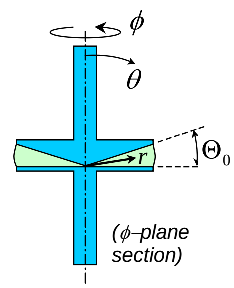

51

Result: $$\underline{v} = \begin{pmatrix} 0 \\ 0 \\ \frac{r\Omega}{\Theta_0}\left(\frac{\pi}{2}-\theta\right) \end{pmatrix}_{r\theta\phi}$$ $\dot{\gamma} = \frac{\Omega}{\Theta_0} =$ constant

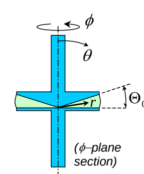

Note: The shear rate is a constant.

The extra stresses τ_{ij} are only a function of the shear rate, thus the τ_{ij} are constant as well.

$$\underline{\underline{\tau}} = \begin{pmatrix} \tau_{rr} & 0 & 0 \\ 0 & \tau_{\theta\theta} & \tau_{\theta\phi} \\ 0 & \tau_{\phi\theta} & \tau_{\phi\phi} \end{pmatrix}_{r\theta\phi}$$

(viscometric flow)

Result: $\tau_{ij} =$ constant

Assume:
- Form of velocity
- no ϕ-dependence
- no slip
- isothermal

Torsional cone and plate is a homogeneous shear flow.

52

Result:

$$\tau_{\theta\phi} = C$$

The experimentally measurable variable is the torque to turn the cone:

$$\underline{T} = \iint_S \left[\underline{R} \times \left(\hat{n} \cdot -\underline{\underline{\Pi}} \right) \right]_{surface} dS$$

$$\underline{T} = \int_0^{2\pi} \int_0^{R} \left[r\hat{e}_r \times \left(-\hat{e}_\theta \cdot -\underline{\underline{\Pi}} \right) \right]_{\theta = \frac{\pi}{2}} r\,dr\,d\phi$$

$$T_\theta = T_z = \frac{2\pi R^3 \tau_{\theta\phi}}{3}$$

For an arbitrary fluid, we are able to relate the torque and the shear stress.

53

Torsional Cone-and-Plate Flow - Viscosity

Measureables:
Torque T to turn cone
Rate of angular rotation Ω

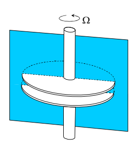

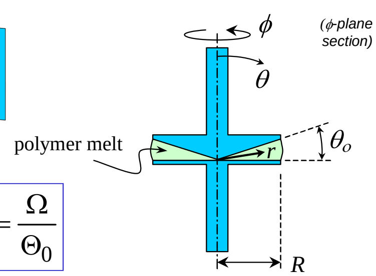

The introduction of the cone means that shear rate is independent of r.

$$\dot{\gamma} = \frac{\Omega}{\Theta_0}$$

Since shear rate is constant everywhere, so is extra stress, and we can calculate stress from torque.

$$\tau_{\theta\phi} = \text{constant} = \frac{3T}{2\pi R^3}$$

$$\eta(\dot{\gamma}) = \frac{3T\Theta_0}{2\pi R^3 \Omega}$$

No corrections needed in cone-and-plate

(and no material assumptions)

54

To calculate normal stresses, look at EOM:

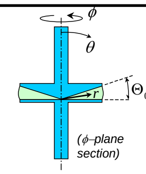

$$P \equiv p - \rho g z$$

$$\rho\left(\cancel{\frac{\partial \underline{v}}{\partial t}} + \cancel{\underline{v}\cdot\nabla\underline{v}}\right) = -\nabla P - \nabla\cdot\underline{\underline{\tau}}$$

steady state

neglect inertia

Also, the pressure is not constant

Although the stress is constant, there are some non-zero terms in the divergence of the stress in the rθϕ coordinate system

$$\underline{\underline{\tau}} = \begin{pmatrix} \tau_{rr} & 0 & 0 \\ 0 & \tau_{\theta\theta} & \tau_{\theta\phi} \\ 0 & \tau_{\phi\theta} & \tau_{\phi\phi} \end{pmatrix}_{r\theta\phi}$$

(viscometric flow)

$$\begin{pmatrix} 0 \\ 0 \\ 0 \end{pmatrix}_{r\theta\phi} = \begin{pmatrix} -\frac{\partial P}{\partial r} \\ -\frac{1}{r}\frac{\partial P}{\partial \theta} \\ 0 \end{pmatrix}_{r\theta\phi} - \begin{pmatrix} \frac{1}{r^2}\frac{\partial r^2\tau_{rr}}{\partial r} - \frac{\tau_{\theta\theta}+\tau_{\phi\phi}}{r} \\ \frac{1}{r\sin\theta}\frac{\partial \tau_{\theta\theta}\sin\theta}{\partial\theta} - \frac{\tau_{\phi\phi}\cot\theta}{r} \\ \frac{1}{r\sin\theta}\frac{\partial \tau_{\theta\phi}\sin\theta}{\partial\theta} + \frac{\tau_{\phi\theta}\cot\theta}{r} \end{pmatrix}_{r\theta\phi}$$

Assume:
- Form of velocity
- no ϕ-dependence
- symmetric stress tensor
- neglect inertia
- no slip
- isothermal

55

On the bottom plate, *sin*θ=1, *cos*θ=0:

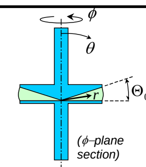

$$\begin{pmatrix} 0 \\ 0 \\ 0 \end{pmatrix}_{r\theta\phi} = \begin{pmatrix} -\frac{\partial P}{\partial r} \\ -\frac{1}{r}\frac{\partial P}{\partial \theta} \\ 0 \end{pmatrix}_{r\theta\phi} - \begin{pmatrix} \frac{2\tau_{rr}}{r} - \frac{\tau_{\theta\theta}+\tau_{\phi\phi}}{r} \\ 0 \\ 0 \end{pmatrix}_{r\theta\phi}$$

$$0 = -\frac{\partial P}{\partial r} - \frac{2\tau_{rr}}{r} + \frac{\tau_{\theta\theta}+\tau_{\phi\phi}}{r}$$

$$0 = -\frac{\partial (P+\tau_{\theta\theta})}{\partial r} - \frac{2\tau_{rr}}{r} + \frac{\tau_{\theta\theta}+\tau_{\phi\phi}}{r}$$ (valid to insert, since extra stress is constant)

$$-\Psi_1\dot{\gamma}_0^2 = \tau_{\phi\phi} - \tau_{\theta\theta}$$
$$-\Psi_2\dot{\gamma}_0^2 = \tau_{\theta\theta} - \tau_{rr}$$
(by definition)

$$\boxed{\frac{\partial \Pi_{\theta\theta}}{\partial \ln r} = -\dot{\gamma}_0^2\left(\Psi_1 + 2\Psi_2\right)}$$

56

Result: $$\boxed{\frac{\partial \Pi_{\theta\theta}}{\partial \ln r} = -\dot{\gamma}_0^2\left(\Psi_1 + 2\Psi_2\right)}$$

The experimentally measurable variable is the fluid thrust on the plate minus the thrust of P_{atm}:

$$N = F_z - \pi R^2 P_{atm}$$

$$\underline{F} = \iint_S \left[\left(\hat{n}\cdot -\underline{\underline{\Pi}}\right)\right]_{surface} dS$$

$$\underline{F} = \int_0^{2\pi}\int_0^R \left[\left(-\hat{e}_\theta \cdot -\underline{\underline{\Pi}}\right)\right]_{\theta=\frac{\pi}{2}} r dr d\phi$$

$$F_\theta = F_z = 2\pi \int_0^R \Pi_{\theta\theta}\big|_{\theta=\frac{\pi}{2}} r dr$$

57

Integrate:

$$\frac{\partial \Pi_{\theta\theta}}{\partial \ln r} = -\dot{\gamma}_0^2\left(\Psi_1 + 2\Psi_2\right)$$

$$\Pi_{\theta\theta} = -\dot{\gamma}_0^2\left(\Psi_1 + 2\Psi_2\right)\ln r + C$$

Boundary condition:

$r = R$

$$\Pi_{\theta\theta} = P_{atm} + \tau_{\theta\theta}\big|_R$$

$$= P_{atm} \underbrace{- \Psi_2\dot{\gamma}_0^2 + \tau_{RR}}_{\text{Directly from definition of } \Psi_2}$$

$$\Pi_{\theta\theta} = -\dot{\gamma}_0^2\left(\Psi_1 + 2\Psi_2\right)\ln\frac{r}{R} + P_{atm} - \Psi_2\dot{\gamma}_0^2$$

$$N = F_z - \pi R^2 P_{atm}$$

$$N = 2\pi \int_0^R \Pi_{\theta\theta}\big|_{\theta=\frac{\pi}{2}} r dr - -\pi R^2 P_{atm}$$

...

58

Torsional Cone-and-Plate Flow – 1st Normal Stress

Measureables:
Normal thrust **F**

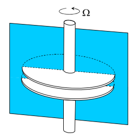

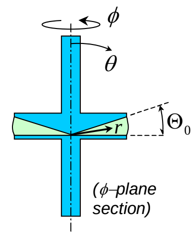

$$N = \left[2\pi \int_0^R \Pi_{\theta\theta}\Big|_{\theta=\frac{\pi}{2}} r\,dr \right] - \pi R^2 p_{atm}$$

The total upward thrust of the cone can be related directly to the first normal stress coefficient.

$$\Psi_1(\dot{\gamma}) = \frac{2F\Theta_0^2}{\pi R^2 \Omega^2}$$

(see also DPL pp522)

59

Torsional Cone-and-Plate Flow – 2nd Normal Stress

$$\Pi_{\theta\theta} = -\dot{\gamma}_0^2 \left(\Psi_1 + 2\Psi_2 \right) \ln \frac{r}{R} + P_{atm} - \Psi_2 \dot{\gamma}_0^2$$

If we obtain $\Pi_{\theta\theta}$ as a function of r / R, we can also obtain Ψ_2.

- MEMS used to manufacture sensors at different radial positions

The Normal Stress Sensor System (NSS)

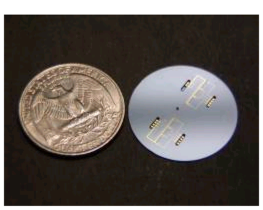

Patented Technology

RheoSense Incorporated
(www.rheosense.com)

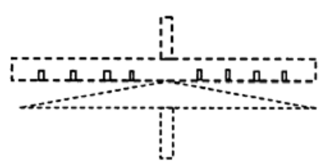

- S. G. Baek and J. J. Magda, J. Rheology, 47(5), 1249-1260 (2003)
- J. Magda et al. Proc. XIV International Congress on Rheology, Seoul, 2004.

60

RheoSense Incorporated

Comparison with other instruments

Monolithic rheometer plate fabricated using silicon micromachining technology and containing miniature pressure sensors for N_1 and N_2 measurements

Seong-Gi Baek[a]

RheoSense, Incorporated, 2357 Ventura Drive, Suite 104, St. Paul, Minnesota 55125

Jules J. Magda

Department of Chemical and Fuels Engineering, University of Utah, 50 South Central Campus Drive, Room 3290, Salt Lake City, Utah 84112

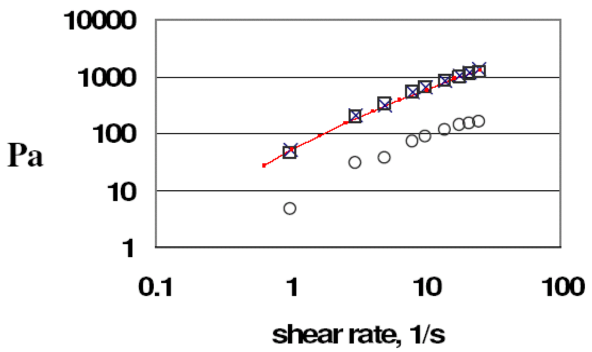

S. G. Baek and J. J. Magda, J. Rheology, 47(5), 1249-1260 (2003)

Treated in detail in Macosko, pp 188-205

Couette Flow (1890)

- Tangential annular flow
- Cup and Bob geometry

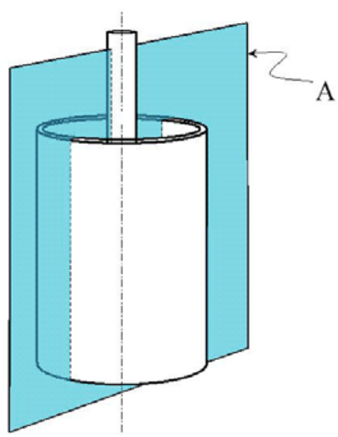

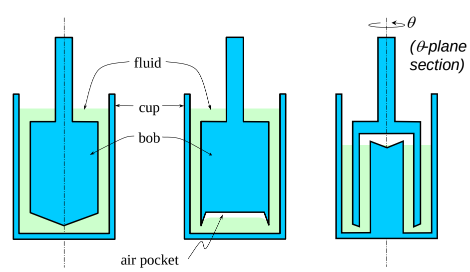

Assume:
- Form of velocity
- no θ-dependence
- symmetric stress tensor
- Neglect gravity
- Neglect end effects
- no slip
- isothermal

Macosko, Rheology: *Principles, Measurements, and Applications*, VCH 1994.

Couette Flow

Assume:
- Form of velocity
- no θ-dependence
- symmetric stress tensor
- Neglect gravity
- Neglect end effects
- no slip
- isothermal

$$\eta = \frac{T(\kappa - 1)}{2\pi R^2 L \kappa^3 \Omega}$$

$$\kappa = \frac{R_{inner}}{R_{outer}}$$

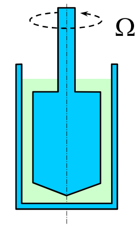

As with many measurement systems, the assumptions made in the analysis do not always hold:

- End effects are not negligible
- Wall slip occurs with many systems
- Inertia is not always negligible
- Secondary flows occur (cup turning is more stable than bob turning to inertial instabilities; there are elastic instabilities; there are viscous heating instabilities)
- Alignment is important
- Viscous heating occurs
- Methods for measuring Ψ_1 are error prone
- Cannot measure Ψ_2

BUT
- Generates a lot of signal
- Can go to high shear rates
- Is widely available
- Is well understood

Macosko, Rheology: *Principles, Measurements, and Applications*, VCH 1994.

63

For the PP and CP geometries, we can also calculate *G'*, *G"*:

Parallel plate

$$\eta'(\omega) = \frac{G''(\omega)}{\omega} = \frac{2HT_0 \sin\delta}{\pi R^4 \omega \theta_0}$$

$$\eta''(\omega) = \frac{G'(\omega)}{\omega} = \frac{2HT_0 \cos\delta}{\pi R^4 \omega \theta_0}$$

Amplitude of oscillation

Cone and plate

$$\eta'(\omega) = \frac{3\Theta_0 T_0 \sin\delta}{2\pi R^3 \omega \phi_0}$$

$$\eta''(\omega) = \frac{3\Theta_0 T_0 \cos\delta}{2\pi R^3 \omega \phi_0}$$

Amplitude of oscillation

- A typical diameter is between 8 and 25mm; 30-40mm are also used
- To increase accuracy, larger plates (R larger) are used for less viscous materials to generate more torque.
- Amplitude may also be increased to increase torque
- A complete analysis of SAOS in the Couette geometry is given in Sections 8.4.2-3

64

Limits on Measurements: Flow instabilities in rheology

Cone and plate/Parallel plate flow

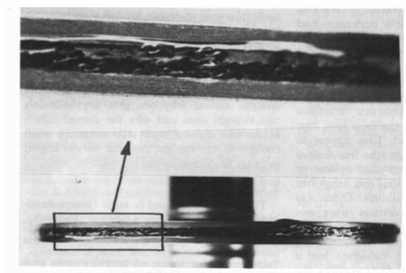

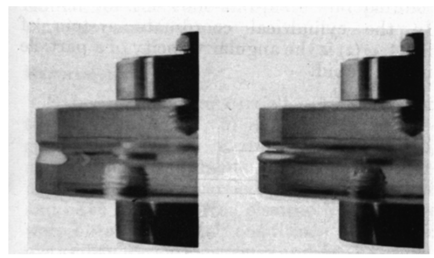

Figures 6.7 and 6.8, p. 175 Hutton; PDMS

65

Limits on Measurements: Flow instabilities in rheology

Taylor-Couette flow

1923 GI Taylor; inertial instability
1990 Ron Larson, Eric Shaqfeh, Susan Muller; elastic instability

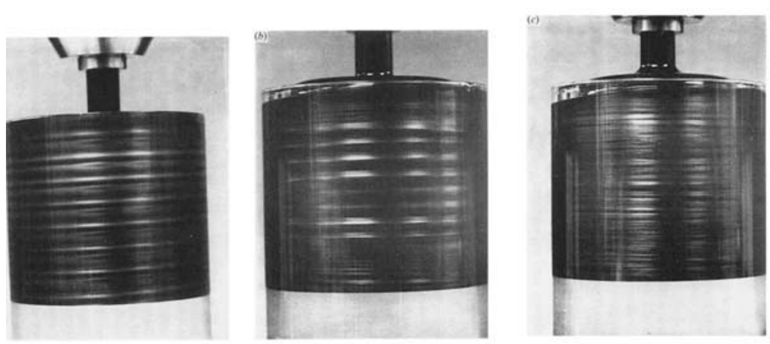

FIGURE 11. Flow visualizations in a Taylor-Couette cell. (*a*) Newtonian fluid at high Taylor number ($Ta = 3800$); (*b*) Boger fluid at negligible Taylor number ($Ta = 9.6\times10^{-4}$) shortly after the onset of secondary flow (t_2 in figure 9); (*c*) Boger fluid at negligible Taylor number after full development of secondary flow (t_3 in figure 9).

- GI Taylor "Stability of a viscous liquid contained between two rotating cylinders," *Phil. Trans. R. Soc. Lond*. A 223, 289 (1923)
- Larson, Shaqfeh, Muller, “A purely elastic instability in Taylor-Couette flow,” *J. Fluid Mech*, 218, 573 (1990)

66

Why do we need more than one method of measuring viscosity?

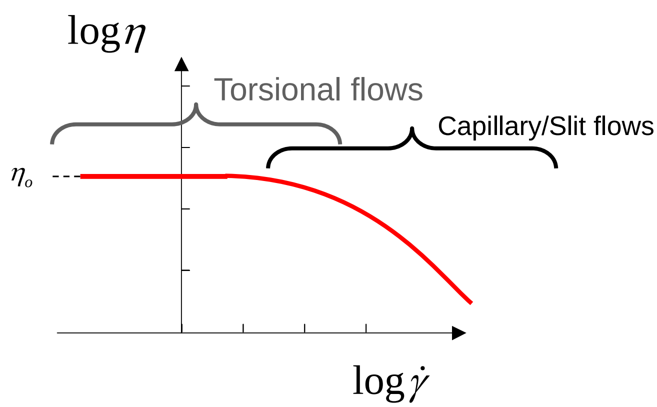

- At low rates, torques/pressures become low
- At high rates, torques/pressures become high; flow instabilities set in

67

Shear measurement

Material Function Calculations

TABLE 10.2
Summary of the Expressions for Steady Shear Rheological Quantities for Common Geometries*

Geometry	Magnitude of Shear Stress $\lvert\tau_{21}\rvert$	Shear Rate $\dot{\gamma}$	Measured Material Function
Capillary flow (wall conditions) $\mathcal{P}_0, \mathcal{P}_L =$ modified pressure at $z = 0, L$ $Q =$ flow rate $L =$ capillary length $\mathcal{R} = \frac{1}{4}\left[3 + \frac{d \ln(4Q/\pi R^3)}{d \ln \tau_R}\right]$ $\tau_R = \tau_{rz}\rvert_{r=R}$	$\frac{(\mathcal{P}_0 - \mathcal{P}_L)R}{2L}$	$\frac{4Q}{\pi R^3}\mathcal{R}$	$\eta = \frac{\tau_R}{4Q/\pi R^3}\mathcal{R}^{-1}$
Parallel disk (at rim) $\mathcal{T} =$ torque on top plate $\Omega =$ angular velocity of top plate, > 0 $H =$ gap $\mathcal{R} = \frac{1}{4}\left[3 + \frac{d \ln(\mathcal{T}/2\pi R^3)}{d \ln \dot{\gamma}_R}\right]$ $\dot{\gamma}_R = \dot{\gamma}(R)$	$\frac{2\mathcal{T}}{\pi R^3}\mathcal{R}$	$\frac{r\Omega}{H}$	$\eta = \frac{2\mathcal{T}}{\pi R^3 \dot{\gamma}_R}\mathcal{R}$
Cone and plate $\mathcal{T} =$ torque on plate $\mathcal{F} =$ thrust on plate $\Omega =$ angular velocity of cone, > 0 $\Theta_0 =$ cone angle	$\frac{3\mathcal{T}}{2\pi R^3}$	$\frac{\Omega}{\Theta_0}$	$\eta = \frac{3\mathcal{T}\Theta_0}{2\pi R^3 \Omega}$ $\Psi_1 = \frac{2\mathcal{F}\Theta_0^2}{\pi R^2 \Omega^2}$
Couette (bob turning) $\mathcal{T} =$ torque on inner cylinder, < 0 $\Omega =$ angular velocity of bob, > 0 $R =$ outer radius $\kappa R =$ inner radius $L =$ length of bob	$\frac{-\mathcal{T}}{2\pi R^2 L \kappa^2}$	$\frac{\kappa\Omega}{1-\kappa}$	$\eta = \frac{\mathcal{T}(\kappa - 1)}{2\pi R^2 L \kappa^3 \Omega}$
Couette (cup turning) $\mathcal{T} =$ torque on inner cylinder, > 0 $\Omega =$ angular velocity of cup, > 0 $R =$ outer radius $\kappa R =$ inner radius $L =$ length of bob	$\frac{\mathcal{T}}{2\pi R^2 L \kappa^2}$	$\frac{\kappa\Omega}{1-\kappa}$	$\eta = \frac{\mathcal{T}(1-\kappa)}{2\pi R^2 L \kappa^3 \Omega}$

* R is radius of fixture. To calculate strain in each case, multiply shear rate by time t. Note that $\eta \equiv -\tau_{21}/\dot{\gamma}_0 = \lvert\tau_{21}\rvert/\dot{\gamma}$.

See also Macosko, Part II

Shear measurements
Pros and Cons

TABLE 10.3
Comparison of Experimental Features of Four Common Shear Geometries

Feature	Parallel Disk	Cone and Plate	Capillary	Couette (Cup and Bob)
Stress range	Good for high viscosity	Good for high viscosity	Good for high viscosities	Good for low viscosities
Flow stability	Edge fracture at modest rates	Edge fracture at modest rates	Melt fracture at very high rates, i.e., distorted extrudates and pressure fluctuations are observed	Taylor cells are observed at high Re due to inertia; elastic cells are observed at high De
Sample size and sample loading	< 1 g; easy to load	< 1 g; highly viscous materials can be difficult to load	40 g minimum; easy to load	10–20 g; highly viscous materials can be difficult to load
Data handling	Correction on shear rate needs to be applied; this correction is ignored in most commercial software packages	Straightforward	Multiple corrections need to be applied	Straightforward
Homogeneous?	No; shear rate and shear stress vary with radius	Yes (small core angles)	No; shear rate and shear stress vary with radius	Yes (narrow gap)
Pressure effects	None	None	High pressures in reservoir cause problems with compressibility of melt	None
Shear rates	Maximum shear rate is limited by edge fracture; usually cannot obtain shear-thinning data	Maximum shear rate is limited by edge fracture; usually cannot obtain shear-thinning data	Very high rates accessible	Maximum shear rate is limited by sample leaving cup due to either inertia or elastic effects; also 3-D secondary flows develop (instability)
Special features	Good for stiff samples, even gels; wide range of temperatures possible	Ψ_1 measurable; wide range of temperatures possible	Constant-Q or constant-$\Delta\mathcal{P}$ modes available; wide range of temperatures possible	Narrow gap required; usually limited to modest temperatures (e.g., $0 < T < 60°C$)

69

Stress/Strain Driven Drag
Multipurpose rheometers

TA Instruments

Anton Paar

Malvern

Thermo Scientific

Brookfield

ATS RheoSystems

Pressure-driven Shear

Göttfert

Instron

ATS RheoSystems

Malvern

(capillary, slit flow; melts)

RheoSense, Inc.

(Slit flow; microfluidics)

Optical

LS Instruments

(diffusive wave spectroscopy; G'G")

(plus attachments on multipurpose rheometer)

Interfacial Rheology

Anton Paar

TA Instruments

BiolinScientific

(drag flow on interface)

70

Elongational Flow Measurements

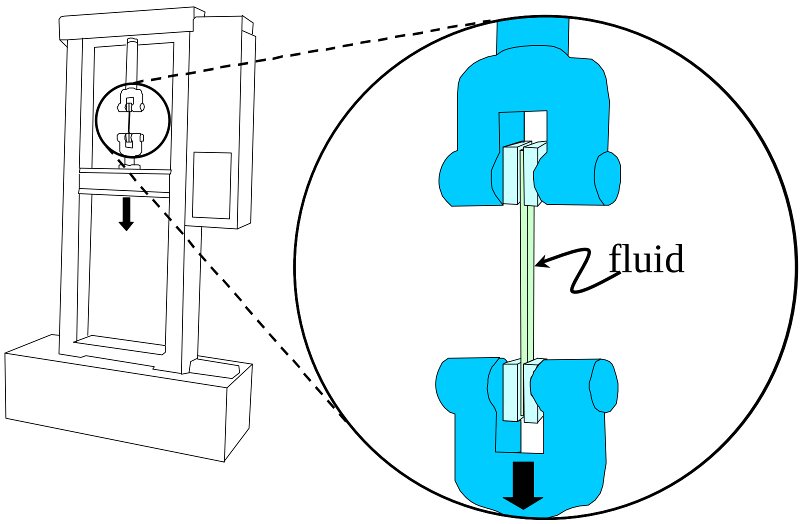

71

Experimental Elongational Geometries

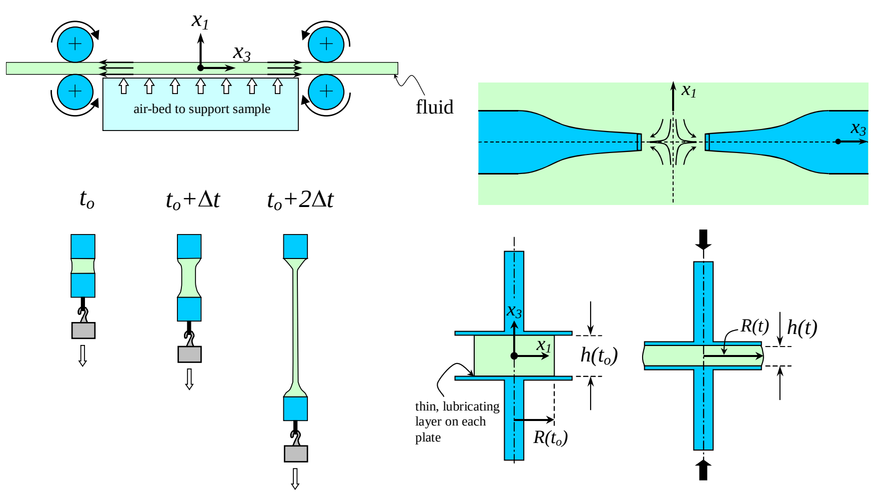

72

Uniaxial Extension

$$\tau_{zz} - \tau_{rr} = -\frac{f(t)}{A(t)}$$

tensile force

time-dependent cross-sectional area

For homogeneous flow: $A(t) = A_0 e^{-\dot{\varepsilon}_0 t}$

$$\boxed{\bar{\eta} = \frac{-(\tau_{zz} - \tau_{rr})}{\dot{\varepsilon}_0} = \frac{f(t_\infty) e^{\dot{\varepsilon}_0 t_\infty}}{A_0 \dot{\varepsilon}_0}}$$

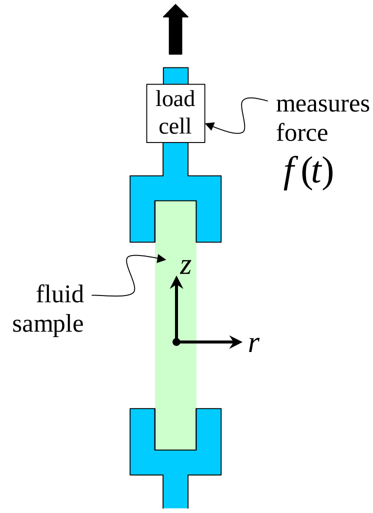

73

Experimental Difficulties in Elongational Flow

ideal elongational deformation

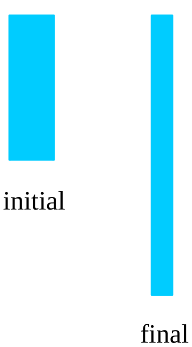

experimental challenges

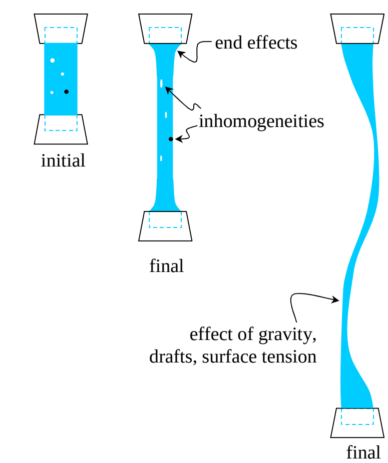

74

Filament Stretching Rheometer (FiSER)

Tirtaatmadja and Sridhar, J. Rheol., 37, 1081-1102 (1993)

- Optically monitor the midpoint size
- Very susceptible to environment
- End Effects

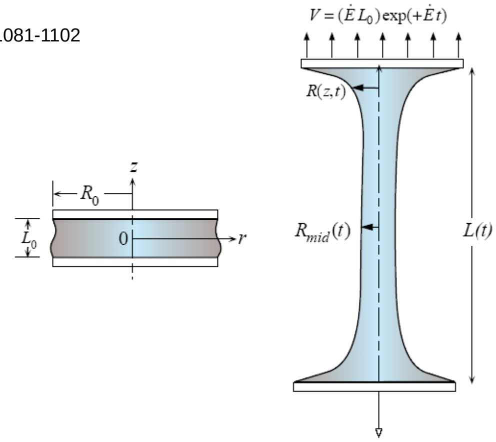

McKinley, et al., 15th Annual Meeting of the International Polymer Processing Society, June 1999.

75

Filament Stretching Rheometer

(Design based on Tirtaatmadja and Sridhar)

"The test sample (a) undergoing investigation is placed between two parallel, circular discs (b) and (c) with diameter $2R_0$=9 mm. The upper disc is attached to a movable sled (d), while the lower disc is in contact with a weight cell (e). The upper sled is driven by a motor (f), which also drives a mid-sled placed between the upper sled and the weight cell; two timing belts (g) are used for transferring momentum from the motor to the sleds. The two toothed wheels (h), driving the timing belts have a 1:2 diameter ratio, ensuring that the mid-sled always drives at half the speed of the upper sled. This means that if the mid-sled is placed in the middle between the upper and the lower disc at the beginning of an experiment, it will always stay midway between the discs. On the mid-sled, a laser (i) is placed for measuring the diameter of the mid-filament at all times.

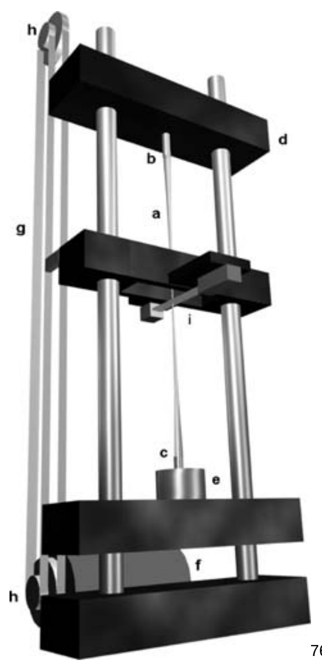

Bach, Rasmussen, Longin, Hassager, JNNFM 108, 163 (2002)

76

Rheol Acta (2001) 40: 457–466

ORIGINAL CONTRIBUTION

Jonathan S. Schulze
Timothy P. Lodge
Christopher W. Macosko
Jens Hepperle
Helmut Münstedt
Heike Bastian
Dino Ferri
David J. Groves
Yong Hoon Kim
Mike Lyon
Thomas Schweizer
Terry Virkler
Erik Wassner
Wim Zoetelief

A comparison of extensional viscosity measurements from various RME rheometers

- Steady and startup flow
- Recovery
- Good for melts

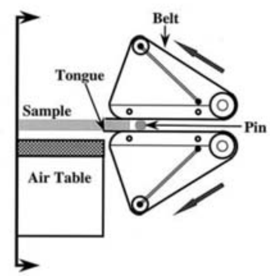

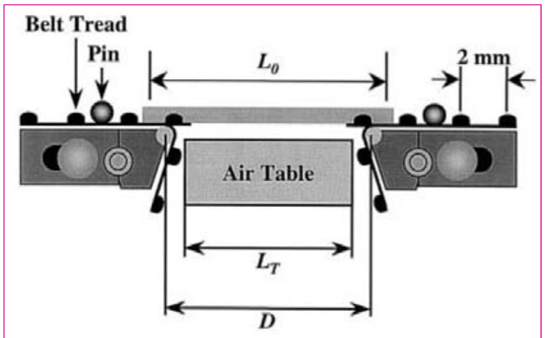

RHEOMETRICS RME 1996 (out of production)

77

Conclusions

Extensional viscosity measurements of a slightly strain hardening LLDPE (Dow Affinity PL 1880) from several Rheometric Scientific RME extensional rheometers were compared with data obtained from the original version of the RME at the ETH Institut für Polymere in Zürich and the Münstedt Tensile Rheometer (MTR) at the University of Erlangen. In general, the commercial RMEs extended samples with a strain rate that was significantly less than the set strain rate. The problem worsened at the higher strain rates of 1.0 s^{-1} and 0.1 s^{-1}, where the difference was at least 10%. The data from the commercial RMEs typically agree with the MTR and original RME within 20%, after the extensional viscosity is corrected for the strain rate.

Achieving commanded strain requires great care.

increased from 50 mm to 60 mm, the deviation in the strain rate decreased from 20% to 2–6%. The recommended value of L_0 should be determined by measuring the distance D and using Eq. (4). However, operating the RME with the correct value of L_0 does not eliminate entirely the strain rate deviation. Based on the performance of earlier rotary clamp rheometers, the strain rate deviation most likely occurs because the velocity of the belts is not sufficiently transferred to the sample during the test. Clearly, the deformation of all materials must be monitored with a video camera, and analyzed to obtain the true strain rate applied to the sample during the test.

Extensional ... improved at al

Use of the video camera (although tedious) is recommended in order to get correct strain rate.

78

Sentmanat Extension Rheometer (2005)

- •Originally developed for rubbers, good for melts
- •Measures elongational viscosity, startup, other material functions
- •Two counter-rotating drums
- •Easy to load; reproducible

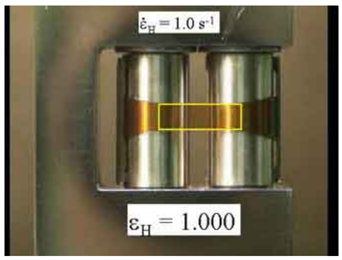

www.xpansioninstruments.com

http://www.xpansioninstruments.com/rheo-optics.htm

79

Sentmanat et al., J. Rheol., 49(3) 585 (2005)

Comparison on different host instruments

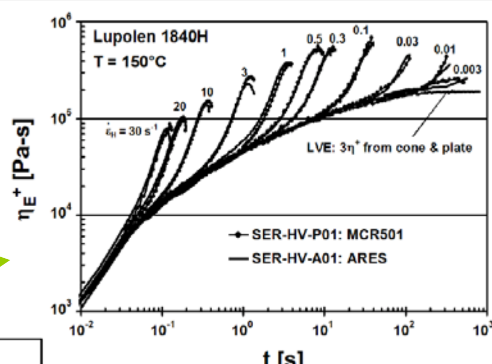

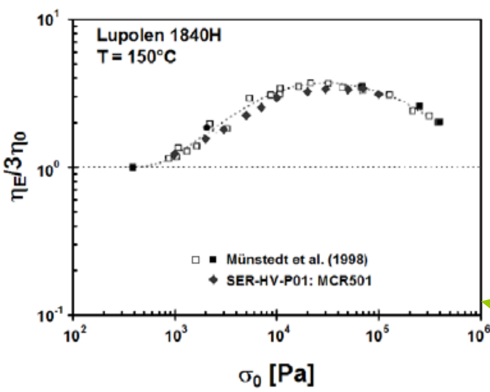

Comparison with other instruments (literature)

80

CaBER Extensional Rheometer

- •Polymer solutions
- •Works on the principle of capillary filament break up
- •Cambridge Polymer Group and HAAKE

For more on theory see: campoly.com/notes/007.pdf

Brochure: www.thermo.com/com/cda/product/detail/1,,17848,00.html

Operation

- •Impose a rapid step elongation
- •form a fluid filament, which continues to deform
- •flow driven by surface tension
- •also affected by viscosity, elasticity, and mass transfer
- •measure midpoint diameter as a function of time
- •Use force balance on filament to back out an apparent elongational viscosity

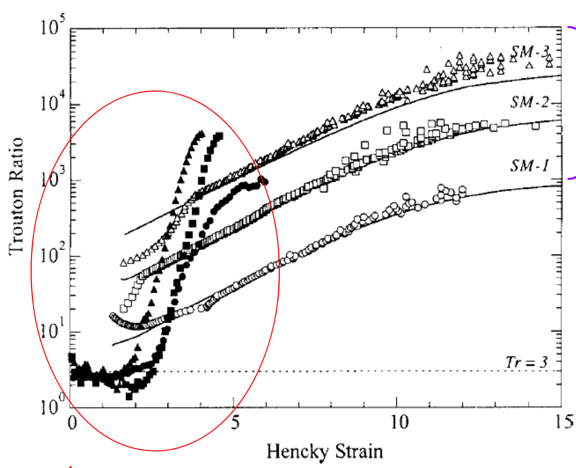

Capillary breakup experiments

Filament stretching apparatus

Comments

- •Must know surface tension
- •Transient agreement is poor
- •Steady state agreement is acceptable
- •Be aware of effect modeling assumptions on reported results

Anna and McKinley, J. Rheol. 45, 115 (2001).

Elongational Viscosity via Contraction Flow: Cogswell/Binding Analysis

Fluid elements along the centerline undergo considerable elongational flow

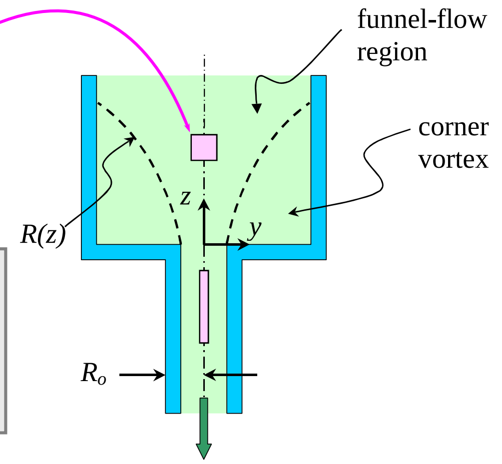

By making strong assumptions about the flow we can relate the pressure drop across the contraction to an elongational viscosity

This flow is produced in some capillary rheometers:

$$\frac{P_{reservoir}-P_{atm}}{L} = \frac{\Delta P_{entrance}}{L} + \frac{\Delta P_{true}}{L}$$

We can use this "discarded" measurement to rank elongational properties

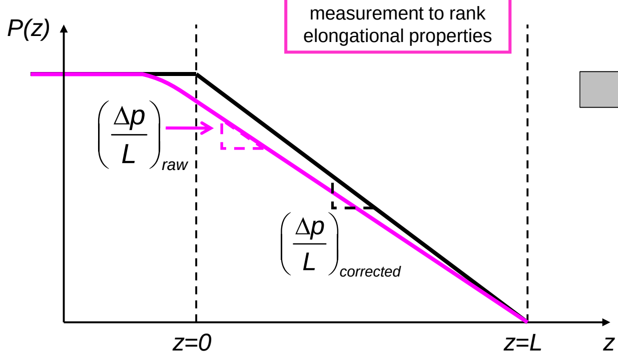

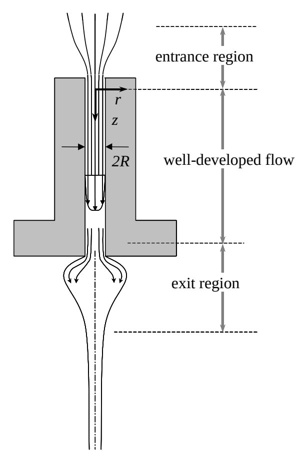

Bagley Plot

$$\Delta P_{\substack{end\\effects}} = f(Q) = f(\dot{\gamma}_a)$$

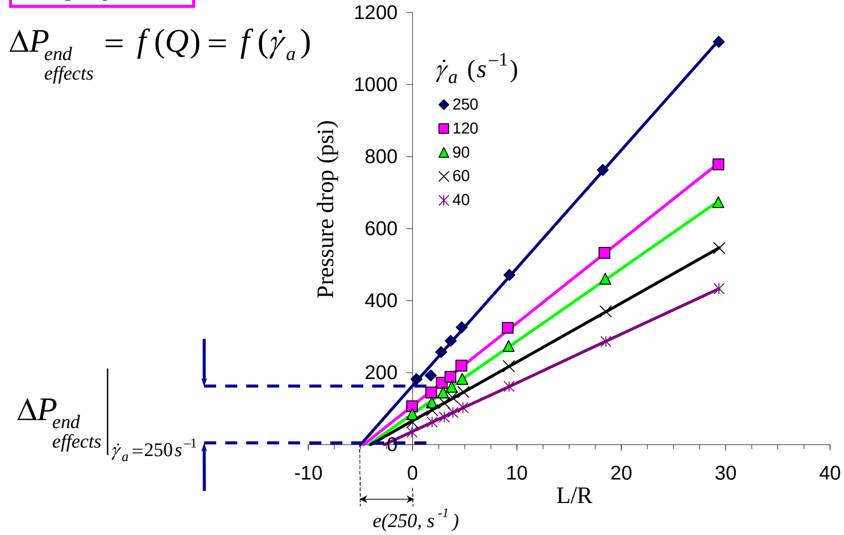

Figure 10.8, p. 394 Bagley, PE

85

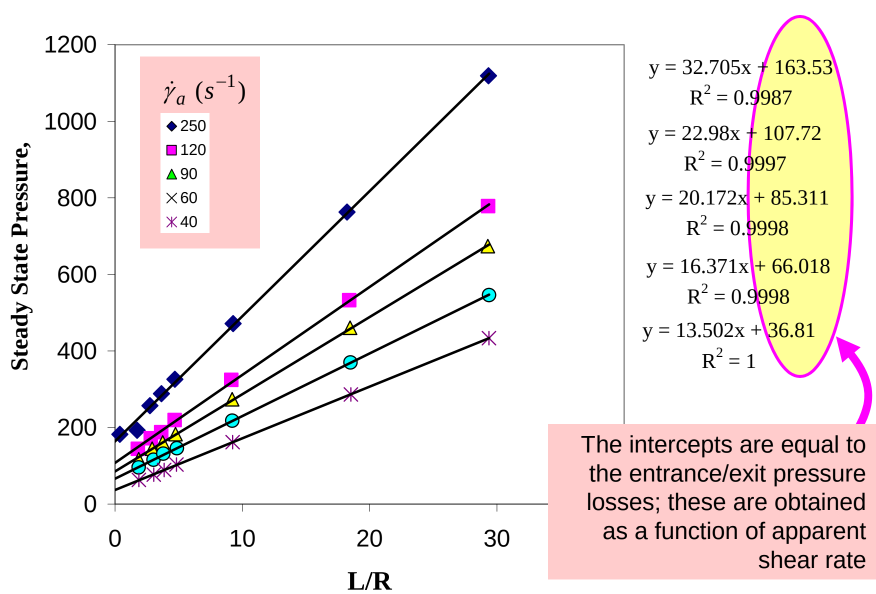

Figure 10.8, p. 394 Bagley, PE

86

Assumptions for the Cogswell Analysis

- incompressible fluid
- funnel-shaped flow; no-slip on funnel surface
- unidirectional flow in the funnel region
- well developed flow upstream and downstream
- θ-symmetry
- pressure drops due to shear and elongation may be calculated separately and summed to give the total entrance pressure-loss
- neglect Weissenberg-Rabinowitsch correction
- shear stress is related to shear-rate through a power-law
- elongational viscosity is constant
- shape of the funnel is determined by the minimum generated pressure drop
- no effect of elasticity (shear normal stresses neglected)
- neglect inertia

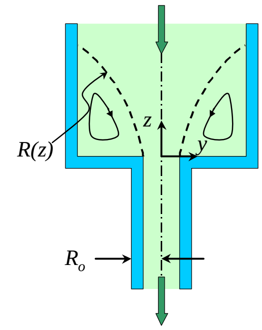

$$\dot{\gamma} \approx \dot{\gamma}_a$$

$$\tau_R = m\dot{\gamma}_a^n$$

$$\bar{\eta} = \text{constant}$$

F. N. Cogswell, Polym. Eng. Sci. (1972) 12, 64-73.
F. N. Cogswell, Trans. Soc. Rheol. (1972) 16, 383-403.

Cogswell Analysis

elongation rate

$$\dot{\varepsilon}_o = \frac{\tau_R \dot{\gamma}_a}{2(\tau_{11} - \tau_{22})}$$

$$\tau_R = \eta\, \dot{\gamma}_a \qquad \eta = m\dot{\gamma}_a^{n-1}$$

$$\dot{\gamma}_a = \frac{4Q}{\pi R^3}$$

elongation normal stress

$$(\tau_{11} - \tau_{22}) = -\frac{3}{8}\Delta p_{ent} \quad (n+1)$$

elongation viscosity

$$\boxed{\bar{\eta} \approx \frac{-(\tau_{11} - \tau_{22})}{\dot{\varepsilon}_o} = \frac{\frac{9}{32}(n+1)^2 \Delta p_{ent}^2}{\tau_R \dot{\gamma}_a}}$$

Cogswell Analysis – using Excel

From shear:

$$\eta = m\dot{\gamma}_a^{n-1}$$

(Binding's data)

$$\dot{\varepsilon}_o = \frac{\tau_R \dot{\gamma}_a}{2(\tau_{11}-\tau_{22})}$$

$$\bar{\eta} = \frac{-(\tau_{11}-\tau_{22})}{\dot{\varepsilon}_o}$$

$$3\eta$$

$$\dot{\gamma}_a = \frac{4Q}{\pi R^3} \qquad \Delta p_{ent} \qquad \Delta p_{ent} \qquad \tau_R$$

RAW DATA gammdotA	RAW DATA deltPent(psi)	deltPent(Pa)	sh stress(Pa)	N1(Pa)	e_rate	Cogswell elongvisc	Cogswell 3*shearVisc
250	163.53	1.13E+06	1.13E+05	-6.27E+05	2.25E+01	2.79E+04	1.55E+03
120	107.72	7.43E+05	7.92E+04	-4.13E+05	1.15E+01	3.59E+04	2.27E+03
90	85.311	5.88E+05	6.95E+04	-3.27E+05	9.56E+00	3.42E+04	2.65E+03
60	66.018	4.55E+05	5.64E+04	-2.53E+05	6.69E+00	3.79E+04	3.23E+03
40	36.81	2.54E+05	4.65E+04	-1.41E+05	6.59E+00	2.14E+04	4.00E+03

$$(\tau_{11}-\tau_{22}) = -\frac{3}{8}\Delta p_{ent}(n+1)$$

Results in one data point for elongational viscosity for each entrance pressure loss (i.e. each apparent shear rate)

Assumptions for the Binding Analysis

- incompressible fluid
- funnel-shaped flow; no-slip on funnel surface
- unidirectional flow in the funnel region
- well developed flow upstream and downstream
- θ -symmetry
- shear viscosity is related to shear-rate through a power-law
- elongational viscosity is given by a power law
- shape of the funnel is determined by the minimum work to drive flow
- no effect of elasticity (shear normal stresses neglected)
- the quantities $(dR/dz)^2$ and d^2R/dz^2, related to the shape of the funnel, are neglected; implies that the radial velocity is neglected when calculating the rate of deformation
- neglect energy required to maintain the corner circulation
- neglect inertia

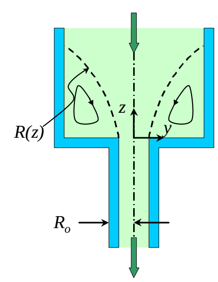

$$\tau_R = m\dot{\gamma}_a^n$$

$$\bar{\eta} = l\dot{\varepsilon}_o^{t-1}$$

D. M. Binding, JNNFM (1988) 27, 173-189.

Binding Analysis

l, elongational prefactor

$$\Delta p_{ent} = \frac{2m(1+t)^2}{3t^2(1+n)^2}\left\{\frac{lt(3n+1)n^t I_{nt}}{m}\right\}^{1/(1+t)} \dot{\gamma}_{R_o}^{\ t(n+1)/(1+t)}\left\{1-\alpha^{3t(n+1)/(1+t)}\right\}$$

$$I_{nt} = \int_0^1 \left| 2 - \left(\frac{3n+1}{n}\right)\phi^{1+1/n}\right|^{t+1} \phi \, d\phi$$

$$\eta = m\dot{\gamma}_a^{n-1}$$

$$\dot{\gamma}_{R_o} = \frac{(3n+1)}{n\pi R_o^3} Q$$

elongation viscosity $\eta = l\dot{\varepsilon}_o^{t-1}$

91

Binding Analysis

Note: there is a non-iterative solution method described in the text; The method using Solver is preferable, since it uses all the data in finding optimal values of l and t.

Evaluation Procedure

1. Shear power-law parameter n must be known; must have data for Δp_{ent} versus Q
2. Guess t, l
3. Evaluate I_{nt} by numerical integration over ϕ
4. Using Solver, find the best values of t and l that are consistent with the Δp_{ent} versus Q data

Results in values of t, l for a model (power-law)

92

Binding Analysis – using Excel Solver

$$I_{nt} = \int_0^1 \left| 2 - \left(\frac{3n+1}{n} \right) \phi^{1+1/n} \right|^{t+1} \phi \, d\phi$$

Evaluate integral numerically

phi	f(phi)	areas
0	0	
0.005	0.023746502	5.93663E-05
0.01	0.047492829	0.000178098
0.015	0.071238512	0.000296828
0.02	0.094982739	0.000415553
0.025	0.118724352	0.000534268
0.03	0.142461832	0.000652965
0.035	0.166193303	0.000771638
0.04	0.189916517	0.000890275
0.045	0.213628861	0.001008863
0.05	0.237327345	0.001127391
0.055	0.261008606	0.00124584
0.06	0.2846689	0.001364194
0.065	0.308304107	0.001482433

. . .

$$area = \frac{1}{2}(b_1 + b_2)h$$

Summing:

Int=	1.36055

93

Binding Analysis – using Excel Solver

Optimize t, l using Solver

By varying these cells:

$$\frac{(predicted - actual)^2}{(actual)^2}$$

t_guess=	1.2477157	
l_guess=	11991.60895	
******* SOLVER SOLUTION ********		
predicted DeltaPent	exptal DeltaPent	difference
1.26E+06	1.13E+06	1.35E-02
6.88E+05	7.43E+05	5.51E-03
5.43E+05	5.88E+05	6.02E-03
3.89E+05	4.55E+05	2.14E-02
2.78E+05	2.54E+05	9.28E-03
	target cell	5.57E-02

Sum of the differences:
Minimize this cell

94

Example calculation from Bagley's Data

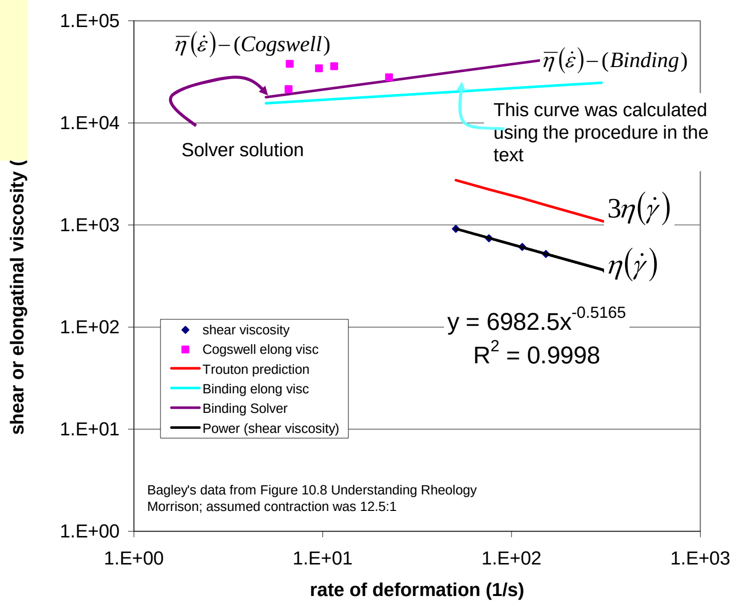

95

Rheotens (Goettfert)

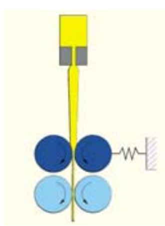

from their brochure:

"Rheotens test is a rather complicated function of the characteristics of the polymer, dimensions of the capillary, length of the spin line and of the extrusion history"

www.goettfert.com/downloads/Rheotens_eng.pdf

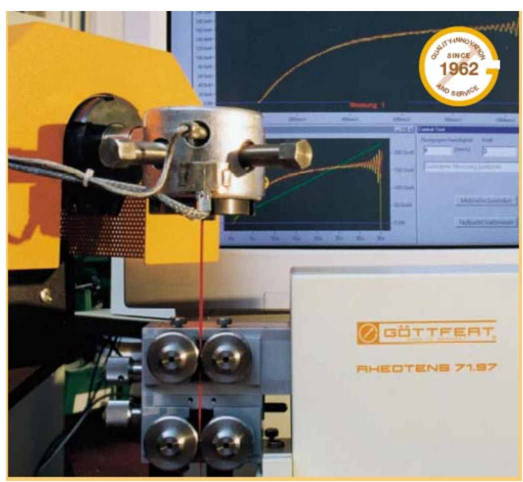

•Does not measure material functions without constitutive model
•small changes in material properties are reflected in curves
•easy to use
•excellent reproducibility
•models fiber spinning, film casting
•widespread application

96

An elongational viscosity may be extracted from a "grand master curve" under some conditions

"The rheology of the rheotens test," M.H. Wagner, A. Bernnat, and V. Schulze, J. Rheol. 42, 917 (1998)

Raw data

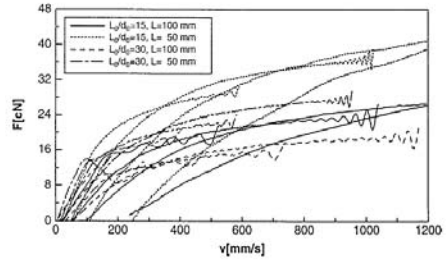

Grand master curve

$b = \text{shift factor}$

Draw resonance

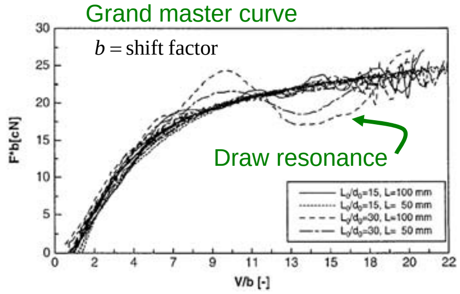

vs. draw ratio $V = v/v_{\text{die exit}}$

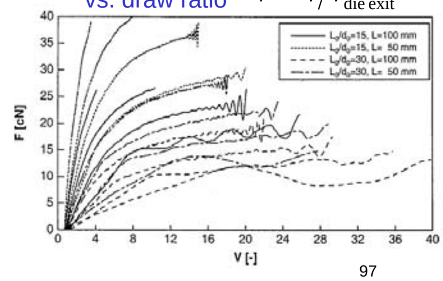

97

Elongational measurements
Pros and Cons

TABLE 10.6
A Comparison of Experimental Features of Four Elongational Geometries

Feature	Melt Stretching	MBER	Filament Stretching	Binding/ Cogswell
Stress Range	Good for high viscosity	Good for high viscosity	Good for low viscosity at room temperature	Good for high and low viscosities
Flow stability	Subject to gravity, surface tension and air currents	Can be unstable at high rates	Subject to gravity, surface tension and air currents	Unstable at very high rates
Sample size and sample loading	10 g; care must be taken to minimize end effects	<2 g; requires careful preparation and loading	<1 g; easy to load	40 g minimum; easy to load
Data handling	Straightforward, but does not result in any elongational material functions	Straightforward; more involved if strain is measured	Two tests are required to account for strain inhomogeneities	Cogswell—straightforward Binding—more complicated but not difficult
Homogeneous?	No, not at ends	Could be with care	No, not at ends	No—mixed shear and elongational flow
Pressure effects	No	No	No	Yes—compressibility of melt reservoir could cause difficulties
Elongation rates	Maximum rates depend on clamp speeds	Maximum elongation rate is limited by ability to maintain the sample in steady flow	Maximum rates depend on plate speeds; minimum rates depend on the ratio of gravity and viscous effects	High and low rates possible
Special features	Cannot reach high strains or steady state; wide range of temperatures is possible; the instrument is commercially available	Often strain is not measured but is calculated from the imposed strain rate; a wide range of temperatures is possible; the instrument is commercially available	Currently limited to room temperature liquids	Is based on a presumed funnel-shaped flow—this may not take place; wide range of temperatures possible

Extensional

Xpansion Instruments
Xpand Your Capabilities
(dual drum windup)

Cambridge Polymer Group, Inc
(filament stretching)

Thermo SCIENTIFIC
(capillary breakup)

TA Instruments
(drum windup)

Measurement of elongational viscosity is still a labor of love.

99

Newer emphasis:

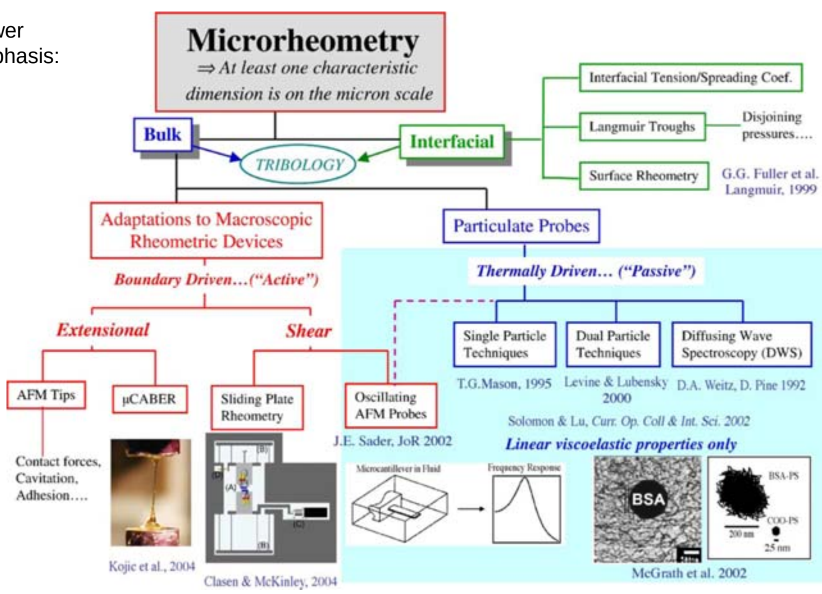

C. Clasen and G. H. McKinley, "Gap-dependent microrheometry of complex liquids," JNNFM, 124(1-3), 1-10 (2004)

100

http://www.ksvnima.com/file/ksv-nima-isrbrochure.pdf

BiolinScientific

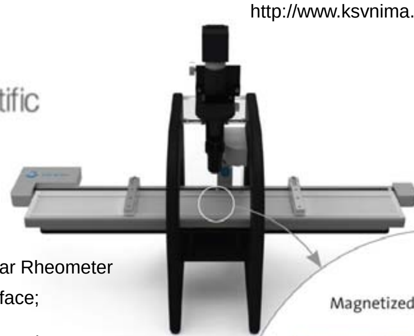

KSV NIMA Interfacial Shear Rheometer

- a probe floats on an interface;
- is driven magnetically;
- material functions are inferred.

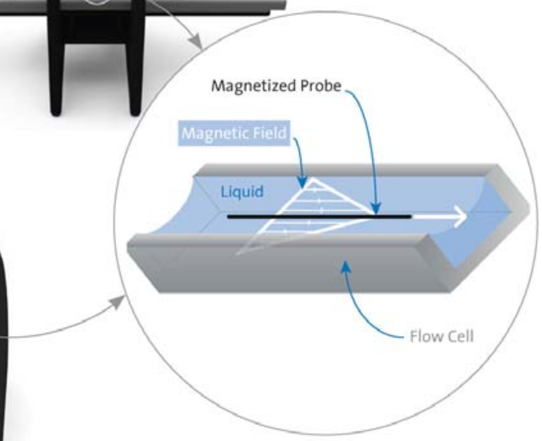

LSinstruments

Contact | Disclaimer | Impressum

Company | Products | Technology | Services | Customers | Applications | Scattering Calculator | Distributors

Diffusing Wave Spectroscopy (DWS)
Dynamic Light Scattering (DLS)
Static Light Scattering (SLS)
Cross Correlation Technologies
Small Angle Light Scattering
Slide Shows

Diffusing Wave Spectroscopy: Microrheology

Diffusing wave spectroscopy (DWS) is an **optical rheology** technique used to obtain viscoelastic properties without ever touching the sample. Instead of applying shear to it, as is done by mechanical rheometers, the sample is illuminated with laser light. After the incoming light has been scattered many times, the resulting intensity fluctuations are detected and the **mean square displacement** of the scattering particles is obtained from this. Principles of **microrheology** are then applied to determine viscous and elastic properties of the sample. What is so exciting about the technique is its ability to measure **storage and loss modulus** [G', G''] within minutes in a huge frequency range.

102

www.lsinstruments.ch/technology/diffusing_wave_spectroscopy_dws/

VOLUME 60, NUMBER 12 PHYSICAL REVIEW LETTERS 21 MARCH 1988

Diffusing-Wave Spectroscopy

D. J. Pine,[1,2] D. A. Weitz,[1] P. M. Chaikin,[1,3] and E. Herbolzheimer[1]
[1]*Exxon Research and Engineering, Annandale, New Jersey 08801*
[2]*Department of Physics, Haverford College, Haverford, Pennsylvania 19041*
[3]*Department of Physics, University of Pennsylvania, Philadelphia, Pennsylvania 19104*
(Received 26 October 1987)

We obtain useful information from the intensity autocorrelations of light scattered from systems which exhibit strong multiple scattering. A phenomenological model, which exploits the diffusive nature of the transport of light, is shown to be in excellent agreement with experimental data for several different scattering geometries. The dependence on geometry provides an important experimental control over the time scale probed. We call this technique diffusing-wave spectroscopy, and illustrate its utility by studying diffusion in a strongly interacting colloidal glass.

PACS numbers: 42.20.Ji, 05.40.+j

Strong multiple scattering of light + model = rheological material functions

•D.J. Pine, D.A. Weitz, P.M. Chaikin, and E. Herbolzheimer,"Diffusing-Wave Spectroscopy," *Phys. Rev. Lett*. 60, 1134-1137 (1988).
•Bicout, D., and Maynard, R., "Diffusing wave spectroscopy in inhomogeneous flows," *J. Phys. I* 4, 387–411. 1993

103

Flow Birefringence - a non-invasive way to measure stresses

no net force, isotropic chain,
isotropic polarization

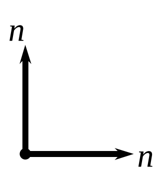

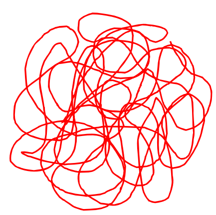

For many polymers, stress and refractive-index tensors are coaxial (same principal axes):

$$\underline{\underline{n}} = C\underline{\underline{\tau}} + B\underline{\underline{I}}$$

Stress-Optical Law

force applied, anisotropic chain,
anisotropic polarization = *birefringent*

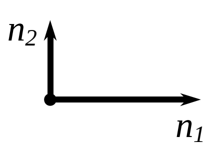

104

Large-Amplitude Oscillatory Shear

A window into nonlinear viscoelasticity

Linear Viscoelasticity & Ellipses

- The equation for a linear viscoelastic response can be re-written (by eliminating time t) to show that the Lissajous figure for stress is **elliptical** when represented vs. shear strain or shear-rate.

$\gamma(t) = \gamma_0 \sin\omega t$ $\qquad \tau = \gamma_0\left[G' \sin\omega t + G'' \cos\omega t\right]$

$$\boxed{\tau^2 - 2G'\tau\,\gamma + \gamma^2\left(G'^2 + G''^2\right) = \left(G''\gamma_0\right)^2}$$

Jules Lissajous (1822-1880)

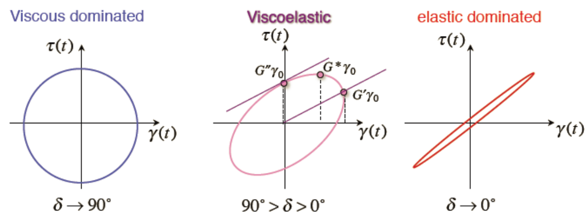

- For further reading, see Wikipedia, Wolfram Mathworld or http://ibiblio.org/e-notes/Lis/Lissa.htm

6

Gareth McKinley, Plenary, International Congress on Rheology, Lisbon, August, 2012
http://web.mit.edu/nnf/ICR2012/ICR_LAOS_McKinley_For%20Distribution.pdf

105

Summary

SHEAR

•Shear measurements are readily made
•Choice of shear geometry is driven by fluid properties, shear rates
•Care must be taken with automated instruments (nonlinear response, instrument inertia, resonance, motor dynamics, modeling assumptions)

•Microrheometry

ELONGATION

•Elongational properties are still not routine
•Newer instruments (Sentmanat,CaBER) have improved the possibility of routine elongational flow measurements
•Some measurements are best left to the researchers dedicated to them due to complexity (FiSER)
•Industries that rely on elongational flow properties (fiber spinning, foods) have developed their own ranking tests

106

Summary

CM4650
Polymer Rheology
Michigan Tech

1. Introduction
2. Math review
3. Newtonian Fluids
4. Standard Flows
5. Material Functions
6. Experimental Data
7. Generalized Newtonian Fluids
8. Memory: Linear Viscoelastic Models
9. Advanced Constitutive Models
10. Rheometry